

1     **Tectonic and climatic controls on fan systems: the Kohrud**  
2                             **mountain belt, Central Iran**

3

4                             Stuart J. Jones<sup>1\*</sup>, Nasser Arzani<sup>2</sup>, Mark B. Allen<sup>1</sup>

5

6     <sup>1</sup>Department of Earth Sciences, Durham University, South Road, Durham, DH1 3LE,

7

UK

8

<sup>2</sup>Geology Department, Payme Noor University, Tehran, Iran

9

10                             \*e-mail: [stuart.jones@durham.ac.uk](mailto:stuart.jones@durham.ac.uk)

11

12 **Abstract**

13 Late Pleistocene to Holocene fans of the Kohrud mountain belt (Central Iran) illustrate  
14 the problems of differentiating tectonic and climatic drivers for the sedimentary  
15 signatures of alluvial fan successions. It is widely recognised that tectonic processes  
16 create the topography that causes fan development. The existence and position of fans  
17 along the Kohrud mountain belt, NE of Esfahan, are controlled by faulting along the  
18 Qom-Zefreh fault system and associated fault zones. These faults display moderate  
19 amounts of historical and instrumental seismicity, and so may be considered to be  
20 tectonically active. However, fluvial systems on the fans are currently incising in  
21 response to low Gavkhoni playa lake levels since the mid-Holocene, producing incised  
22 gullies on the fans up to 30 m deep. These gullies expose an interdigitation of lake  
23 deposits (dominated by fine-grained silts and clays with evaporites) and coarse gravels  
24 that characterise the alluvial fan sediments. The boundaries of each facies are mostly  
25 sharp, with fan sediments superimposed on lake sediments with little to no evidence of  
26 reworking. In turn, anhydrite-glauberite, mirabilite and halite crusts drape over the  
27 gravels, recording a rapid return to still water, shallow ephemeral saline lake  
28 sedimentation. Neither transition can be explained by adjustment of the hinterland  
29 drainage system after tectonic uplift. The potential influence in central Iran of enhanced  
30 monsoons, the northward drift of the Intertropical Convergence Zone (ITCZ) and  
31 Mediterranean climates for the early Holocene (~6–10 ka) point to episodic rainfall  
32 (during winter months) associated with discrete high magnitude floods on the fan  
33 surfaces. The fan sediments were deposited under the general influence of a highstand

34 playa lake whose level was fluctuating in response to climate. This study demonstrates  
35 that although tectonism can induce fan development, it is the sensitive balance between  
36 aridity and humidity resulting from changes in the climate regime of central Iran that  
37 influences the nature of fan sequences and how they interrelate to associated facies.

38

39 Keywords: alluvial fans, climate, tectonism, central Iran, playa lakes, ITCZ

40

## 41 **1. Introduction**

42 The association between active faults and alluvial fans is well established in the  
43 research literature (e.g., Allen and Hovius, 1998; Jones, 2004; Harvey 2012; Bahrami,  
44 2013). Moreover, fluvial-fans (megafans), alluvial fans and fan deltas have been widely  
45 documented from the margins of many ancient and recent depositional basins in  
46 extensional (Gawthorpe and Leeder, 2000; Leeder and Mack, 2001), transtensional  
47 (Dorsey, 2002; Sözbilir et al., 2011; Le Dortz et al., 2011) and compressional tectonic  
48 settings (Jones, 2004; Leleu et al., 2009; Waters et al., 2010). In many modern  
49 structurally active areas it is very tempting to interpret any cyclical or episodic  
50 sedimentation as tectonically controlled. In such settings an important question is  
51 whether or not the character of the alluvial fan sediments and sequences can be used to  
52 assess the degree and rate of fault activity (e.g., Ford et al., 1997; Quigley et al., 2007).

53 It is clear that tectonism provides the opportunity for alluvial fan development  
54 through creation of topography, increasing gradients of river systems supplying  
55 sediments, and creating accommodation space for storage of sediment. Tectonic

56 activity has a fundamental control on fan development, of any size (Blair and  
57 McPherson, 1994; Allen and Hovius, 1998; Jones, 2004). However, the influx of coarse  
58 clastic sediment alone cannot be taken as direct evidence of fault activity and  
59 rejuvenation of a drainage basin.

60 Our hypothesis is that climatically controlled events can produce sedimentary  
61 signatures similar to those created by tectonism and individual fault activity (Pope and  
62 Wilkinson, 2005; Waters et al., 2010). In fact it is well known in arid zones that small  
63 changes in rainfall can have pronounced and even devastating effects on river  
64 discharge, and therefore sediment supply and lake levels within intermontane basins  
65 (Vázquez-Urbez et al., 2013). In addition there are low frequency/high magnitude flood  
66 events associated with enhanced monsoon and seasonal winter rainfall due to ITCZ  
67 migration that lead to substantial runoff (e.g., Frostick and Jones 2002). All of these  
68 affect the development and character of sediments on alluvial fans (e.g. Walker and  
69 Fattahi, 2011; Arzani, 2012).

70 This paper will firstly summarise the general geology and geomorphology of  
71 the study area based on satellite imagery, digital topography, geology maps and our  
72 own detailed fieldwork observations. We then describe the alluvial fan sedimentology,  
73 proximal fan hot-spring intercalated travertines and distal intercalated playa lake  
74 sediments which are all part of the distal alluvial fan system. Finally, we use a variety  
75 of published age constraints from periods of Late Pleistocene and early Holocene fan  
76 abandonment from central and eastern Iran, to constrain the timing and controls on the

77 alluvial fans draining the southwestern side of the Kohrud Mountain belt of central  
78 Iran, an area never previously studied in detail.

79

## 80 **2. Geological Setting**

81 The Iranian Plateau is a relatively flat area whose morphology strongly contrasts to that  
82 of the mountains to the south (Zagros) and to the north (Alborz and Kopet Dagh). Mean  
83 elevations in the plateau region are typically 1500 – 2000 m asl, in contrast with the  
84 desert lowlands of the Dasht-e Kavir and Dasht-e Lut to the east (Fig. 1), which are  
85 <1000 m asl. The plateau includes regions with more pronounced topography such as  
86 the NW-SE trending Urumieh-Dokhtar Zone, which is largely formed by an Eocene  
87 magmatic arc. The Iranian Plateau is a sector of the larger Turkish-Iranian Plateau, that  
88 covers ~1.5 million km<sup>2</sup> in area (Fig. 1).

89 Iran has a complex tectonic history that involves closure of minor ocean basins  
90 (Berberian, 1981), which originally separated microcontinental blocks. Precambrian to  
91 Carboniferous strata of these microcontinents are very similar, indicating that they once  
92 formed part of a broad platform on the eastern margin of Gondwana (Scotese and  
93 McKerrow, 1990; Heydari et al., 2003). Permian rifting was responsible for the  
94 separation and northward motion of the Iranian microcontinents away from Arabia.  
95 Collision with Eurasia took place during Middle-Late Triassic time (Berberian, 1981;  
96 Davoudzadeh, 1997; Stampfli et al., 1991). By the Jurassic a subduction zone  
97 developed along the western edge of the Sanandaj-Sirjan Zone (Fig. 1), and the  
98 Urumieh-Dokhtar magmatic arc began to form (Alavi, 1994; Berberian, 1981). Initial

99 collision of Arabia and Eurasia took place at ~35 Ma, in the late Eocene (Allen and  
100 Armstrong, 2008), and convergence has continued to the present (Agard et al., 2005).

101 A major tectonic re-organisation at ~5 Ma led to the end of or reduction in slip  
102 on many faults within the Turkish-Iranian Plateau, and the onset of the present  
103 configuration of deformation across a vast area from western Turkey to eastern Iran  
104 (Allen et al., 2004). The precise reason for this re-organisation is not clear, but crustal  
105 thickening and shortening across an orogenic plateau tends to cease once a critical  
106 elevation threshold is reached (Allen et al., 2013). Seismogenic thrusts within the  
107 Zagros are very rare above elevations of 1250 m (Nissen et al., 2011), although the rise  
108 in elevations above this level indicates that another process must operate to produce the  
109 plateau. Mantle support of central Iran, linked to the scattered Pliocene-Quaternary  
110 magmatism, is possible (Maggi and Priestley, 2005). Other factors linked to the present  
111 high elevations of the plateau may be underthrusting of the Arabian plate beneath Iran  
112 (Paul et al., 2010).

113 At present, limited plate convergence takes place within the Iranian plateau: the  
114 GPS-derived velocity field indicates internal deformation on the scale of 2 mm/yr or  
115 less (Vernant et al., 2004). In contrast, ~20 mm/yr of north-south Arabia-Eurasia  
116 convergence takes place at longitude 51° E (roughly Tehran), but most of this is  
117 achieved within the Zagros to the south of the plateau and the Alborz/Kopet Dagh  
118 ranges and the South Caspian Basin to its north.

119 The study area is located along the central portion of the Urumieh-Dokhtar  
120 Zone, known as the Kohrud mountain belt and the northeastern margin of the Meymeh-

121 Esfahan basin (MEB) of central Iran (Fig. 2). The MEB occupies the northwestern  
122 portion of the larger Gavkhoni-Abarkoh-Sirjan depression (Fig. 1). This depression is  
123 more than 600 km long. The Urumieh-Dokhtar Zone is sliced obliquely by NW-SE or  
124 NNW-SSE trending right-lateral strike-slips faults such as the Qom-Zefreh (Kashan)  
125 and Deh Shir (Meyer et al., 2006; Allen et al., 2011). Offset on these faults is typically  
126 tens of kilometres, and possibly up to 40 km for the Qom-Zefreh Fault (Allen et al.,  
127 2011). These faults may have acted to help accommodate plate convergence by rotating  
128 anti-clockwise about vertical axes, at the same time as lengthening the collision zone  
129 along strike.

130         These faults do not appear to be particularly active compared with many other  
131 structures in Iran: they are not typically associated with instrumental records of  
132 earthquakes of  $M_w \sim 5$  or above (Jackson et al., 1995; Fig. 1) and, as noted above, they  
133 do not perturb the GPS-derived velocity field. However, nor are they completely  
134 inactive: an earthquake in AD 1344 near the southeast end of the Qom-Zefreh Fault  
135 was an estimated  $M \sim 5.7$  (Ambraseys and Melville, 1982), while numerous smaller  
136 earthquakes have been recorded instrumentally (Nadimi and Konon, 2012). Jamali et al.  
137 (2011) recorded offset streams and historical drainage channels (qanats) along the line  
138 of the Qom-Zefreh Fault.

139

### 140 **3. Stratigraphy**

141 The alluvial fans along the northwestern side of the Gavkhoni-Abarkoh-Sirjan  
142 depression have drainage basins carved into the Kohrud mountain belt. These can be

143 separated into two broad terranes divided by the Qom-Zefreh Fault (Fig. 2). In the  
144 northwest fans are sourced largely from drainage basins with Devonian sandstones,  
145 Triassic dolomites, Lower Jurassic sandstones and Lower Cretaceous *Orbitolina*  
146 limestones. This contrasts to fans in the southeast of the study area that have drainage  
147 basins within Middle to Upper Eocene granodiorites, gabbros and volcanics (basaltic-  
148 andesites). Tectonic activity since the mid Tertiary has thrust and uplifted the  
149 successions (Berberian, 1981; Aghanabati, 2004).

150 Late Pliocene to Recent alluvial sediments are found along the margins of the  
151 Kohrud Mountain belt and create an important link between the mountain drainage and  
152 playa lake, as recognised in many other parts of Iran (e.g., Arzani, 2005, 2012; Walker  
153 and Fattahi, 2011; Fig. 3). However, from field observations and drilling in the  
154 Gavkhoni playa, a similar drainage pattern to other playas in central Iran has probably  
155 existed since earlier times (Nadimi and Konon, 2012): Pliocene marls underlie  
156 Quaternary marls and conglomerate intercalations adjacent to the modern lake. The  
157 total Quaternary succession is recorded as >300 m in these places (Nadimi and Konon,  
158 2012). In contrast, the fan sediments are of unknown thickness, but assumed to thicken  
159 closer to the mountain fronts and grade basinwards into evaporites and fine-grained  
160 sediments of the Gavkhoni playa lake (Fig. 3). There is presently ~500 m elevation  
161 difference between the apices of the fans and their toes.

162



163 **4. Hydrology**

164 *Rivers*

165 Modern drainage patterns in central Iran have probably existed very broadly since the  
166 deposition of the Early Miocene Upper Red Formation and its equivalents (Morley et  
167 al., 2009; Ballato et al., 2011). Rivers draining the northern and southern sides of the  
168 MEB have predominately transverse patterns that cut across several basin-bounding  
169 faults and have built large alluvial fans. The fans on the northern side of the basin form  
170 the subject of this study. The Zayandeh Rud (rud = river) flows along the basin axis. In  
171 many places this river cuts the toes of the alluvial fans or captures any associated  
172 drainage (Fig. 2).

173 The present climate of the area is arid to semi-arid with average rainfall ranging  
174 between 50 and 200 mm in the basin, and up to 350 mm in the headwaters of many  
175 rivers of the Kohrud Mountain belt (Alijani et al., 2008). Because of this, all rivers  
176 except the Zayandeh Rud are ephemeral, and most flows occur during the late winter  
177 months and Spring (December to April). A rainfall gradient from the headwaters to the  
178 middle/lower reaches of many streams exists and flow is more likely in the upper  
179 reaches of the rivers.

180

181 *Gavkhoni playa lake*

182 Along the axis of the Gavkhoni-Abarkoh-Sirjan depression (Figs. 1, 2) are several  
183 playa lakes, the floors of which can occur as high as 1500 m asl. Gavkhoni playa lake  
184 itself is at 1450 m asl. All of the playa lakes are hypersaline and at the present day do

185 not contain any water within them for much of the year. High salt concentrations arise  
186 partly from high evaporation rates in this enclosed arid basin. However, significant  
187 recharge comes from the alluvial fan drainage systems that drain Eocene alkali volcanic  
188 terranes, and from relatively high solute loads of the present day axial Zayandeh Rud.

189         It has been widely documented that lake levels of intermontane rift basins are  
190 highly variable (Cross et al., 2000; Magee et al., 2004) and have a considerable  
191 influence over sedimentation and architecture of contemporaneous basin fills (Owen  
192 and Renaut, 1986; Frostick, 1997; Lin et al., 2001). Lake Zeribar and Mirabad in the  
193 Zagros Mountains and Lake Urmia in NW Iran provide lake core records of climate  
194 changes during the Holocene and corresponding lake level changes (e.g. Steven et al.,  
195 2006; Wasylkova et al., 2006; Djamali et al., 2010). The Gavkhoni playa lake (Fig. 2)  
196 will have experienced several rises and falls of the lake levels and had an important  
197 impact on both erosional modification and progradation of the fan systems.

198

## 199 **5. The Esfahan fluvial fan systems**

200 Along the southern side of the Kohrud Mountain belt, between Soh and southeast of  
201 Varzaneh in the MEB (Fig. 2), there are at least 35 fluvial fans of different sizes that  
202 build out from the edge of the mountain front. Some of these fans are sited against  
203 faults at the mountain front (e.g., Zefreh), and may be an indicator of at least some  
204 present fault activity. Others are at places where the mountain front is abrupt, but no  
205 active fault is recognised (e.g., Soh); topography may be relict from late Cenozoic,  
206 when the faulting was more prevalent within the area of the present day plateau.

207 According to the restricted classification of alluvial fans by Blair and  
208 McPherson (1994), the Esfahan fans would be described as fluvial depositional  
209 systems. However, the application of such a rigid classification seems inappropriate  
210 with such well-defined fan geometries (Fig. 2) and the recognition that fans are  
211 controlled by many allocyclic and autocyclic processes (Frostick and Jones, 2002;  
212 Jones, 2004). In this paper the term fluvial fan is used (or *megafan*, as named first by  
213 Gohain and Parkash, 1990) to describe a large ( $10^2$ - $10^3$  km<sup>2</sup>) and gentle low gradient,  
214 fan-shaped sedimentary accumulation formed mostly by fluvial deposits. Usually,  
215 fluvial fans generate from large catchments developed in mountain ranges (Fig. 4); the  
216 majority of the 35 fluvial fans in our study area have catchment areas of 10-10<sup>2</sup> km<sup>2</sup>. By  
217 contrast, alluvial fans are typically smaller in size than fluvial fans, have local  
218 catchments and steeper slopes, with a greater predominance of gravity driven  
219 sedimentary deposits (*sensu* Blair and McPherson, 1994).

220 Of the 35 fluvial fans that build from the flank of the Kohrud towards the  
221 Gavkhoni-Abarkoh-Sirjan depression, three large and by inference long-lived fans were  
222 selected for study. They are (from northeast to southwest): Soh; Zefreh; and Feshark  
223 (Figs. 4 - 6). The Soh fan is the largest with an area of 537 km<sup>2</sup> (Table 1). It also  
224 illustrates some of the best exposures of the fanglomerates. The Soh fan is comparable  
225 to other similar sized fluvial fans along the margin of the basin (e.g., Arzani, 2005,  
226 2012). The Zefreh and Feshark fans are slightly smaller in size with fan areas of 309  
227 km<sup>2</sup> and 179 km<sup>2</sup> respectively (Table 1). The toe of the Soh fan is at 1750 m asl; the  
228 toes of the Zefreh and Feshark fans are at ~1500 m, and on the edge of the Gavkhoni

229 playa (Fig. 2). The fluvial fans in this study provide a useful reference for patterns of  
230 sedimentation and sequential fan development, but are also of use in providing  
231 information about fan evolution in areas of differing catchment geology and,  
232 potentially, base level change (Fig. 2).

233         Like most fan systems worldwide, precise dating of the Esfahan fans is  
234 problematic because of the lack of diagnostic fossils or other material typically used for  
235 radiometric dating. A variety of techniques using cosmogenic nuclide exposure dating,  
236 luminescence dating and uranium series dating has been widely applied to date fan  
237 surfaces and associated cross-cutting faults across central and eastern Iran (Table 2).  
238 The dating of Holocene and Late Pleistocene fan development in the central Iranian  
239 plateau region has allowed the Esfahan fans and landscape development to be  
240 constrained (e.g., Le Dortz et al., 2009; Talebian et al., 2010). The widespread  
241 landscape evolution during the Holocene for the Iranian plateau region sees an  
242 abandonment phase of most of the fan surfaces at ~11 - 9 ka (Walker and Fattahi, 2011;  
243 Table 2). Records of lake and playa highstand sedimentation indicate corresponding  
244 wetter conditions for the Gavkhoni playa at ~9.6 +/- 2.4 ka and for the South Golbah,  
245 SE Iran at 7.9 +/- 0.1 ka (Table 2). These periods of fan activity reflect increased  
246 moisture from the early to mid Holocene, supported by speleothem analysis in Oman  
247 recording a continental pluvial event for the early to middle Holocene at 10.5 - 6 ka  
248 (Burns et al., 2001). Increased aridification since ~6 ka is widely supported across  
249 central Iran from archaeological data (Schmidt et al., 2011) and multi proxy climate  
250 data from several lakes (Stevens et al., 2001; Wasylkova, 2006; Kehl, 2009). The

251 Esfahan fans appear to have been relatively stable since the onset of increased aridity in  
252 the region with no directly attributable fan activity.

253

#### 254 *Fluvial fan geomorphology*

255 The long profiles of each of the fans are an important element of understanding  
256 catchment and fan area evolution in that, together with the channel networks, they fix  
257 the boundary conditions for slope processes (Fig. 7). River long profiles show an  
258 approximately graded profile for each fan and its bedrock catchment area, with a  
259 localised knickpoint at the apex of the Soh fan. The general geometry of the fans  
260 conforms to the classical models of a fan with a conical radiating form (e.g., Bull, 1977;  
261 Stainstreet and McCarthy, 1993). The Soh fan is deeply incised (Fig. 5), which is  
262 probably the result of a combination of tectonic uplift and playa lake level fall. The  
263 Zefreh and Feshark fans are more elongate in plan view than the Soh fan, and lack the  
264 incision of the latter (Fig. 6). In cross-section all of the fans are wedge-shaped and the  
265 latest phase of fan development is also incised. Ayoubi (2002) has dated paleosols from  
266 the margin of the Gavkhoni Playa, that intercalate with the younger alluvial fans  
267 sediments at Zefreh, by optically stimulated luminescence (OSL) as c. 9.6 ka BP (Table  
268 2). Since then a further 10 - 12 m of incision has taken place.

269         Incision of the Soh fan has produced near-vertical cliffs of up to ~30 m in height  
270 (Fig. 8). Individual beds that can be traced over distances > 1 km provide an  
271 opportunity for detailed sections to be studied, allowing for a comprehensive  
272 understanding of fan evolution, architecture and interaction with playa sediments. In

273 general, fans at the northwest end of the MEB tend to be more incised than those to the  
274 southeast. Possibly, their higher elevations make them more prone to incision during  
275 lake level lowstands. The Soh fan is particularly incised, and perhaps effectively  
276 abandoned/beheaded during lowstand phases: the main channel in the vicinity currently  
277 passes immediately to the east of the Soh fan, feeding a newer fan to its east that has  
278 prograded farther into the basin interior (Fig. 5).

279

#### 280 *Fan sediments*

281 The fan sediments are characterized by sheets of polymict, clast- or matrix-supported  
282 conglomerates. The sheets of conglomerate are laterally competent and extend up to  
283 750 m in section, and individual beds range in thickness from 30 cm – 1 m (Fig. 8). The  
284 conglomerates predominantly show a bimodal grain size with predominantly cobble-  
285 grade clasts and a medium-grained to granular sand-grade matrix (Fig. 9). Clasts tend to  
286 be subangular to subrounded. A variety of sedimentary structures is observed  
287 throughout. Large scale planar cross stratification (<1 m) is found in thicker beds  
288 whereas imbrication, incorporated with pebble clustering on bedding surfaces and in  
289 cross section, erosive bases and fining-upward packages are common in most of the  
290 succession (Figs. 8, 9).

291 The fan lithologies strongly reflect their drainage basin geology with the Soh  
292 fan dominated by Devonian, Triassic and Cretaceous limestones and sandstones. This  
293 contrasts to the Zefreh and Feshark fans whose drainage basin geology is located with  
294 in the Urmieh–Dokhtar volcanic belt consisting of volcanoclastics, basaltic and

295 andesitic volcanics (Ghasemi and Talbot, 2006). The predominance of the  
296 volcanoclastic clasts for the Zefreh and Feshark fans (Fig. 9; Table 1), is what provides  
297 their characteristic black colour on Landsat images (Fig. 6).

298 Conglomerates and coarse grained clastics make up approximately 90% of the  
299 observable fan sediments in the proximal regions close to the fault scarp (Fig. 8), but  
300 within ~20 km down fan this has decreased to < 45% (Fig. 10). The remainder of the  
301 sequence is composed of fine-grained playa lake sediments and evaporites. An  
302 exception to the general pattern is the proximal to medial part of the Soh fan. It consists  
303 of predominantly coarse-grained clastics derived from incision of precursor Plio-  
304 Pleistocene fan sediments that prograded at previous playa lake levels. The only fine-  
305 grained playa lake sediments occur as either laterally truncated lens or as thin veneers.  
306 They indicate lacustrine transgressions, but are largely truncated and eroded by  
307 successive later fan flood events.

308 In proximal reaches of the Soh fan and to a lesser extent the Zefreh and Feshark fans,  
309 intercalated hot-spring travertines and travertine-cemented fan conglomerates are a  
310 common associated facies (Fig. 8, 11). The travertines can reach ~3 m thick (Fig. 8)  
311 and extend laterally up to ~450 m. The intercalated travertines tend to be layered mats  
312 composed of alternating layers of porous and dense carbonate horizons (Fig. 11A). The  
313 dense horizons are composed of fine-grained micrite. Thicker micrite horizons  
314 commonly contain angular to sub-rounded clasts of fine to medium-grained detrital  
315 quartz and even small pebbles from the alluvial fan drainage basin lithologies.  
316 Examples of layered mat travertines preserving rim pool structures (or microterrace

317 textures) that occurred on the margins of an ancient travertine mound are less common  
318 and only found in proximal regions of the fans, in close proximity to a fault (Fig. 11B).  
319 Cobble to pebble size conglomerates are frequently cemented by travertine and usually  
320 contain blocks of angular layered mat (Arzani, 2012). Many of the hot-spring travertine  
321 locations along the Urmieh–Dokhtar volcanic belt of the central Iranian plateau are  
322 associated with important Paleolithic sites (Heydari-Guran et al., 2009).

323

#### 324 *Playa lake sediments*

325 The playa lake sediments are commonly red-brown clays with discrete layers of  
326 anhydrite-glauberite, mirabilite and halite, although in the most recent sediments there  
327 are abundant gypsum crystals occurring as layers and within the fine-grained detritus.  
328 The fine grained sediments are derived from the distal parts of the fans that represent  
329 the suspended fraction and downstream fining of high magnitude-low frequency flash  
330 flood events that prograde out into the playa lake (Figs. 12, 13). In addition suspended  
331 sediment carried by the rivers provides an alternative source (Fig. 2). Observations  
332 from the modern playa lake illustrates that the gypsum tends to form as patches and as a  
333 white crust on the surface of the playa during drying out, with no lake level identifiable  
334 (Fig. 14). It is suggested that the evaporites were deposited in quiet, very shallow water  
335 conditions, perhaps where water was pooled at the margins of the playa and evaporites  
336 are intercalated with clastic sediments.



337 Other lesser components of the playa, are polygonal desiccation cracks, mud  
338 curls and thin (maximum of 0.4 m thick) medium-grained sandy stringers. These  
339 features are always found in the distal part of the fans.

340 Gypsiferous marls drape fans at places along the northern side of the MEB at a  
341 consistent elevation of 1600 m asl. A section of these sediments shows as a pale blue  
342 stripe along the Landsat mosaic in Fig. 6, aligned NW-SE. At the same elevation, there  
343 is a 30 m high scarp ~6 km to the east of the modern shoreline of Gavakhoni playa,  
344 likewise draped by a veneer of pale sediments. We interpret these features as the  
345 collective record of a lake highstand, perhaps of early Holocene age, 150 m above the  
346 present playa surface. Walker and Fattahi (2011) recorded relatively wet conditions in  
347 central and eastern Iran about 8 ka BP or younger. Gavkhoni playa lake is about 600  
348 km from the lacustrine strata dated by Walker and Fattahi (2011), and at a similar  
349 latitude, and comparable present-day climate.

350

## 351 **6. Discussion**

### 352 *Tectonic activity*

353 As discussed in section 2, the faults and mountains ranges in the study area are  
354 apparently less active during the Pliocene – Quaternary than earlier times, but they are  
355 not completely inert. It is therefore tempting to speculate that many of the coarse beds  
356 represent tectonically-induced erosion and sediment flux from the hinterland  
357 catchments (e.g., Blair and McPherson 1994; Mack and Leeder, 1999; Viseras et al.,  
358 2003; Allen et al., 2013). An alternative interpretation is that progradation of the fan

359 deposits over the playa lake sediments was caused by a increase in basin subsidence  
360 rate. This process would create coarsening upward successions, but this motif is absent  
361 from the Esfahan fans. The fan deposits mostly have sharp contacts above playa lake  
362 sediments, while conversely the playa lake sediments abruptly drape the fan conglomerates  
363 and finer-grained fan sediments (Figs. 10, 11).

364           However, from satellite images (Figs. 5, 6), field observations and geological  
365 mapping it is evident that tectonics is very important in controlling the gross location of  
366 the fans, including their outlet positioning from the Kohrud mountain front. Several  
367 studies have highlighted the importance of drainage basin scale and fault  
368 locations/orientations in controlling drainage patterns and hence outlet spacing into a  
369 depositional basin (e.g., Hovius, 1996; Jones et al., 2001; Jones, 2004). In this sense,  
370 the Soh, Zefreh and Feshark fan positions are all clearly controlled by tectonism, with  
371 major faults or fault intersections located at or near the apex of the fans (Allen et al.,  
372 2011; Le Dortz et al., 2011; Figs. 2, 5, 6). A landscape dominated by tectonics, rather  
373 than sediment availability and changes in precipitation, will show fluvial incision in  
374 regions of uplift often located close to a fault. It is also obvious that fault activity along  
375 the basin margin controlled hot-spring travertine deposition along fault lines and at  
376 intersections between adjacent fault segments, which locally contributed to fan  
377 deposition. Fault activity may have promoted an increase in hydrothermal groundwater  
378 discharge rates with rapid degassing of CO<sub>2</sub> at or near the surface leading to phases of  
379 travertine precipitation. In many locations up to 20 m of incision has occurred through  
380 hot-spring travertines especially in the proximal portion of the Soh fan (Arzani, 2012;

381 Figs. 5, 8). Tectonic signals may be overprinted by climatic events with higher  
382 frequency and shorter response times (Humphrey and Heller, 1995; Allen and  
383 Densmore, 2000; Allen et al., 2013). Unless tectonic activity manifests itself in  
384 prolonged and drastic landscape modification, climate perturbations will most likely  
385 overprint local or small scale tectonic signals as for the Esfahan fans. Periods of higher  
386 rainfall and infiltration of runoff could have enhanced the hydrothermal circulation and  
387 led to the several phases of travertine precipitation as intercalated amongst the fan  
388 sediments (Fig. 8). We find little geomorphic evidence for the numerous active faults  
389 depicted by Nadimi and Konon (2012) around the present margins of Gavkhoni playa  
390 lake, and suggest these features should be the target of further study.

391

#### 392 *Climatic control on sedimentation*

393 The recognition of climatic signals in sedimentary successions is more difficult than  
394 tectonic signatures due to the timescales over which climate influences sedimentation  
395 and the number of overlapping geomorphic processes that operate with climate  
396 (Frostick and Jones, 2002). However, it is inevitable that any fluctuations in climate  
397 within a drainage system will have a consequent effect on sediment delivery to the  
398 depositional basin (e.g., Huisink, 1997, 1999; Fryirs and Brierley, 1998; Jones et al.,  
399 1999). This is most evident in the Esfahan fans where superposition of coarse-grained  
400 clastics on playa lake sediments, and a recognisable cyclicity in sedimentation, are not  
401 readily attributable to tectonism (Fig. 11).

402           An increase in precipitation in the early Holocene is reflected in playa lake  
403 levels of the Gavkhoni that were at least 150 m above present lake levels (Ayoubi,  
404 2002; Arzani, 2012; Fig. 6). This is consistent with lake deposition in other areas of the  
405 Middle East (Bar-Matthews et al., 2003) and North Africa where the Dead Sea  
406 experienced elevated lake levels in the early Holocene (Frostick and Reid 1989;  
407 Frumkin, 1997; Klinger et al., 2003). Interestingly, the occurrence of a pluvial or a  
408 wetter phase during the early Holocene is not present in lake cores from lake Zeribar  
409 and the nearby lake Mirabad in the Zagros Mountains, and the lake Urmia record from  
410 the NW (Stevens et al., 2006). From oak pollen records a sharp rise is recognized  
411 around ~6 ka that may reflect an increase in moisture content in the mid-Holocene  
412 (Stevens et al., 2006; Wasylkova et al., 2006 ). However, cave speleothem records  
413 from northern Oman show enhanced monsoonal rainfall from ~10.6 ka with a return of  
414 arid conditions by 6.3 ka (e.g. Burns et al., 2001; Fleitmann et al., 2007), and it is  
415 possible that central and southeastern parts of Iran were also subject to monsoonal rains  
416 during the early Holocene (e.g., Regard et al., 2006). The early Holocene wetter period  
417 with fluctuations in playa lake levels (mostly fed by the Zayandeh Rud) accounts for  
418 the transgressive events of lacustrine sediments, but does not necessarily explain why  
419 coarser-grained clastics are interbedded in the playa succession.

420           The simplest and most plausible explanation is that the coarse-grained fan  
421 sediments were laid down by low-frequency, high-magnitude flood events. Temporal  
422 and spatial rainfall variations in arid zones is likely to give rise to infrequent large  
423 floods (Schick and Lekach, 1987) and the high sediment flux resulting from rainfall-

424 runoff processes will supply large amounts of sediment to the alluvial fans (Frostick et  
425 al., 1983; Frostick and Jones, 2002). High magnitude flood events will account for  
426 abrupt contacts with the underlying playa lake sediments and the coarse alluvial  
427 sediments would have been laid down quickly, i.e., one bed per flash flood. However,  
428 perhaps more significantly it accounts for the abrupt change to the unadulterated playa  
429 sediments and finite thickness of each alluvial bed (Figs. 8, 10). There are no  
430 interspersed alluvial fan sediments in the playa lake sediments, or a general fining  
431 tendency that would be expected if the system as a whole were trying to adjust itself to  
432 tectonic rejuvenation.

433         The current semi-arid to arid setting of the central Iranian plateau is located in  
434 the transition zone of the eastern extensions of the winter depressions from the  
435 Mediterranean (Northwesterlies), dominated by winter storm tracks and the north-  
436 western extension of the strong seasonal reversal of the arid winter-NE and the humid  
437 summer-SW (Asian) monsoon (see Fig. 3 in Kober et al., 2013). Any northward shift in  
438 the Intertropical Convergence Zone (ITCZ) during an interglacial period would imply  
439 an enhanced influence of monsoonal rainfall and prevailing pluvial conditions  
440 (Fleitman et al., 2007; Preusser, 2009; Kehl, 2009; Djamali et al., 2010). An alternative  
441 moisture source is by the Mediterranean Northerwesterlies winter rainfall that directs  
442 moisture from the Middle East and Western Asia (Bar-Matthews et al., 1997; Kober et  
443 al., 2013).

444         The potential influence in central Iran of both the Monsoonal and Mediterranean  
445 climates for the early Holocene (~6 – 10 ka) points to episodic rainfall (during winter

446 months) associated with variable magnitude flash floods on the fan surfaces. This  
447 increased episodic rainfall is also likely to be accountable for the hot-spring travertine  
448 deposition seen in the proximal portions of the Esfahan fans (Heydari-Guran et al.,  
449 2009; Arzani, 2012) and for similar age late Pleistocene to early Holocene travertines  
450 of Turkey (e.g., Vermoere et al., 1999).

451         The sensitive balance between aridity and humidity from the interaction  
452 between the Mediterranean, Indian Monsoonal and northward shift of the ITCZ during  
453 the early Holocene pluvial event will have resulted in highly erosive flood events on the  
454 Esfahan fans, liberating significant amounts of sediment that were deposited under the  
455 general influence of a highstand playa lake whose level was fluctuating in response to  
456 climate (rainfall). The consequence was periodic drowning of the fan toes and  
457 accumulation of lake sediments, most of which was derived from a suspended load of  
458 low-magnitude flash floods, but also from evaporite precipitation in the Gavkhoni playa  
459 lake. Sporadically throughout the fan sequence, high magnitude flash floods crossed out  
460 onto the playa lake. The structure and fabric of these sediments is reminiscent of  
461 braided stream deposits of the present day fans. These changes reflect changing patterns  
462 of discharge and sediment availability, in response to early Holocene climatic  
463 fluctuations within the drainage network of the Kohrud Mountain belt.

464

## 465 **7. Conclusions**

466         Although it has been widely recognised that fault movement, fault geometries  
467 and subsidence create a topography that induces fan development, climate exerts a

468 more discrete control on sediments of alluvial fan sequences. This is perhaps too easily  
469 overlooked in both modern and ancient basin settings but, as recognised in this study,  
470 climate is a more important control of alluvial fan sequences once an outlet has been  
471 sited along the mountain front. Tectonic activity tends to be located along major faults  
472 that may dissect fans but do not directly influence the sedimentation.

473         This raises an important question of interpretation of similar deposits in more  
474 ancient successions. Since the sedimentary signature of a climatically driven high-  
475 magnitude flood is the same as that supposed to characterise a post-tectonic flood, there  
476 can be little justification for an automatic assumption that either climate or tectonism  
477 had a greater responsibility for the deposit without corroborating evidence. In fact in  
478 recent years there is a growing number of measurements of the sedimentary effects of  
479 large floods on alluvial fans, and climate is argued as the more important control on  
480 sediment flux and fan evolution (e.g., Quigley et al., 2007; Walker and Fattahi, 2011).

481         This study has demonstrated that although tectonism can induce fan  
482 development, it is the sensitive balance between aridity and humidity resulting from  
483 changes in the climate regime of a region that influences the nature of fan sequences  
484 and how they interrelate to associated facies. This is easily overlooked in the need to  
485 identify tectonic events and interpret ancient basin history.

486

#### 487 **Acknowledgements**

488 We gratefully appreciate field support supplied by the University of Payme Nour, Iran  
489 for SJJ & NA. We would like to thank Brian Turner and Lynne Frostick for critical

490 comments on an earlier version of this paper. Paolo Ballato, an anonymous referee and  
491 the editor Jasper Knight provided very helpful reviews.

492

## 493 **References**

494 Agard, P., Omrani, J., Jolivet, L., Mouthereau, F., 2005. Convergence history across  
495 Zagros (Iran): constraints from collisional and earlier deformation. *International*  
496 *Journal of Earth Sciences* 94, 409-419.

497 Aghanabati, A., 2004. *The Geology of Iran*. Geological Survey of Iran. 389pp.

498 Alavi, M., 1994. Tectonics of the Zagros orogenic belt of Iran: new data and  
499 interpretations. *Tectonophysics* 29, 211-238.

500 Alijani, B., O'Brien, J., Yarnal, B., 2008. Spatial analysis of precipitation intensity and  
501 concentration in Iran. *Theoretical and Applied Climatology* 94, 107-124.

502 Allen, M., Jackson, J., Walker, R., 2004. Late Cenozoic reorganization of the Arabia-  
503 Eurasia collision and the comparison of short-term and long-term deformation rates.  
504 *Tectonics* 23, TC2008, doi: 2010.1029/2003TC001530.

505 Allen, M.B., Armstrong, H.A., 2008. Arabia-Eurasia collision and the forcing of mid  
506 Cenozoic global cooling. *Palaeogeography, Palaeoclimatology, Palaeoecology* 265,  
507 52-58.

508 Allen, M.B., Kheirkhah, M., Emami, M.H., Jones, S.J., 2011. Right-lateral shear across  
509 Iran and kinematic change in the Arabia-Eurasia collision zone, *Geophysical Journal*  
510 *International* 184, 555-574.



511 Allen, M.B., Saville, C., Blanc, E.J-P., Talebian, M., Nissen, E., 2013. Orogenic  
512 plateau growth: expansion of the Turkish-Iranian Plateau across the Zagros fold-and-  
513 thrust belt. *Tectonics* 32, 171-190.

514 Allen, P.A., Hovius, N., 1998. Sediment delivery to basins from landslide driven  
515 fluxes. *Basin Research* 10, 19-35.

516 Allen, P.A., Densmore, A.L., 2000. Sediment flux from an uplifting fault block. *Basin*  
517 *Research* 12, 367–380.

518 Allen, P.A., Armitage, J.A., Carter, A., Duller, R.A., Michael, N.A., Sinclair, H.D.,  
519 Whitchurch, A.L., Whittaker, A.C., 2013. The Qs problem: Sediment volumetric  
520 balance of proximal foreland basin systems. *Sedimentology* 60, 102–130.

521 Ambraseys, N.N., Melville, C.P., 1982. *A History of Persian Earthquakes*, Cambridge  
522 University Press, Cambridge, UK.

523 Arzani, N., 2005. The fluvial megafan of Abarkoh Basin (central Iran): an example of  
524 flash-flood sedimentation in arid lands. In: Harvey, A.M., Mather, A.E., Stokes, M.,  
525 (Eds.), *Alluvial fans: geomorphology, sedimentology, dynamics*. Geological Society  
526 of London Special Publication 251, pp 41-59.

527 Arzani, N., 2012. Catchment lithology as a major control on alluvial megafan  
528 development, Kohrud Mountain range, central Iran. *Earth Surface Processes and*  
529 *Landforms* 37, 726-740.

530 Ayoubi, S., 2002. Pedogenic evidences of Quaternary climate change recorded in  
531 paleosols from Isfahan and Emam-Gheis (Charmahal-Bakhtiari province).  
532 Unpublished Ph.D. thesis. Isfahan University of Technology, Iran.

533 Ballato, M., Uba, C.E., Landgraf, A., Strecker, M.R., Sudo, M., Stockli, D.F., Friedrich,  
534 A., Tabatabaei, S.H., 2011. Arabia-Eurasia continental collision: Insights from late  
535 Tertiary foreland-basin evolution in the Alborz Mountains, northern Iran, Geological  
536 Society of America Bulletin 123, 106-131.

537 Bahrami, S., 2013. Tectonic controls on the morphometry of alluvial fans around  
538 Danekhoshk anticline, Zagros, Iran. *Geomorphology* 180-181, 217-230.

539 Bar-Matthews, M., Ayalon, A., Kaufman, A., 1997. Late Quaternary Paleoclimate in  
540 the Eastern Mediterranean Region from stable isotope analysis of speleothems at  
541 Soreq Cave, Israel. *Quaternary Research* 47, 155–168.

542 Bar-Matthews, M., Ayalon, A., Gilmour, M., Matthews, A., Hawkesworth, C.J., 2003.  
543 Sea-land oxygen isotopic relationships from planktonic foraminifera and speleothems  
544 in the Eastern Mediterranean region and their implication for paleorainfall during  
545 interglacial intervals. *Geochimica et Cosmochimica Acta* 67, 3181-3199.

546 Berberian, M., 1981. Active faulting and tectonics of Iran. *Geological Survey of Iran*  
547 52, 464-500.

548 Blair, T.C., McPherson, J.G., 1994. Alluvial fans and their natural distinction from  
549 rivers based on morphology, hydraulic processes, sedimentary processes and facies  
550 assemblages. *Journal of Sedimentary Research* 64, 450-589.

551 Bull, W.B., 1977. The alluvial fan environment. *Progress in Physical Geography* 1,  
552 222-270.

553 Burns, S.J., Fleitmann, D., Matter, A., Neff, U., Mangini, A., 2001. Speleothem  
554 evidence from Oman for continental pluvial events during interglacial periods.  
555 *Geology* 29, 623–626.

556 Cross, S.L., Baker, P.A., Seltzer, G.O., Fritz, S.C., Dunbar, R.B., 2000. A new  
557 estimate of the Holocene lowstand level of Lake Titicaca and implications for  
558 regional paleohydrology. *The Holocene* 10, 21-32.

559 Djamali, M., Akhiani, H., Andrieu-Ponel, V., Braconnot, P., Brewer, S., de Beaulieu, J.-  
560 L., Fleitmann, D., Fleury, J., Gasse, F., Guibal, F., Jackson, S.T., Lézine, A.-M.,  
561 Médail, F., Ponel, P., Roberts, N., Stevens, L.R., 2010. Indian summer monsoon  
562 variations could have affected the early-Holocene woodland expansion in the Near  
563 East. *The Holocene* 20, 813-820.

564 Davoudzadeh, M., 1997. Geology of Iran. In: Moores, E.M., Fairbridge, R.W. (Eds).,  
565 *Encyclopedia of Asian and European Regional Geology*. Chapman & Hall, London,  
566 pp 384-405.

567 Dorsey, R.J., 2002. Stratigraphic record of Pleistocene initiation and slip on the Coyote  
568 Creek fault, Lower Coyote Creek, southern California. In: Barth, A. (Ed),  
569 *Contributions to Crustal Evolution of the Southwestern United States: Boulder,*  
570 *Colorado*, Geological Society of America Special Paper 365, pp 251–269.

571 Fleitmann, D., Burns, S. J., Mangini, A., Mudelsee, M., Kramers, J., Neff, U., Al-  
572 Subbary, A. A., Matter, A., 2007. Holocene ITCZ and Indian monsoon dynamics  
573 recorded in stalagmites from Oman and Yemen (Socotra). *Quaternary Science*  
574 *Reviews* 26, 170-188.

575 Ford, M., Williams, E.A., Artoni, A., Verges, J., Hardy, S., 1997. Progressive evolution  
576 of a fault-related fold pair from growth strata geometries, Sant Llorens de Morunys,  
577 SE Pyrenees. *Journal of Structural Geology* 19, 413-441.

578 Frostick, L.E., 1997. The East African rift basins. In: Selley, R.C. (Ed), *African Basins.*  
579 *Sedimentary Basins of the World* 3, pp 187-209.

580 Frostick, L.E., Reid, I., Layman, S.T., 1983. Changing size distribution of suspended  
581 sediment in arid-zone flash floods. In: Collinson, J.D, Lewin, J. (Eds), *Modern and*  
582 *Ancient Fluvial Systems.* Special Publication International Association of  
583 *Sedimentologists* 6, pp 97-106.

584 Frostick, L.E., Reid, I., 1989. Climatic versus tectonic controls of fan sequences:  
585 lessons from the Dead Sea, Israel. *Journal Geological Society London* 146, 527-538.

586 Frostick, L.E., Jones, S.J., 2002. Impact of periodicity on sediment flux in alluvial  
587 systems; grain to basin scale. In: Jones, S.J., Frostick, L.E., (Eds), *Sediment supply*  
588 *to basins: causes, controls and consequences.* Geological Society of London Special  
589 *Publication* 191, pp 81-95.

590 Fryirs, K., Brierley, G., 1998. The character and age structure of valley fills in upper  
591 Wolumla Creek catchment, south east, New South Wales, Australia. *Earth Surface*  
592 *Processes and Landforms* 23, 271-287.

593 Ghasemi, A., Talbot, C.J., 2006, A new tectonic scenario for the Sanandaj-Sirjan zone  
594 (Iran). *Journal of Asian Earth Sciences* 26, 683–693.

595 Gawthorpe, R.L., Leeder, M.R., 2000. Tectono-sedimentary evolution of active  
596 extensional basins. *Basin Research* 12, 195-218.

597 Gohain, K., Parkash, B., 1990. Morphology of the Kosi megafan. In: Rachocki, A.H.,  
598 Church, M. (Eds), Alluvial fans: a field approach. Wiley, Chichester, pp 151-178.

599 Harvey, A.M., 2012. The coupling status of alluvial fans and debris cones: a review and  
600 synthesis. *Earth Surface Processes and Landforms* 37, 64–76.

601 Heydari, E., Wade W.J., Ghazi A.M., 2003. Permian Triassic boundary interval in the  
602 Abadeh section of Iran with implications for mass extinction: part 1; *Sedimentology*.  
603 *Palaeogeography, Palaeoclimatology, Palaeoecology* 193, 405-423.

604 Heydari-Guran, S., Ghasidian, E., Conard, N.J., 2009. Paleolithic Sites on Travertine  
605 and Tufa Formations in Iran. In: Otte, M., Biglari, F., Jaubert, J. (Eds)., *Iran*  
606 *Palaeolithic. Proceedings of the XV World Congress UISPP, Lisbonne, 28, BAR*  
607 *International Series* 1968, pp 109-124.

608 Hovius, N., 1996. Regular spacing of drainage outlets from linear mountain belts. *Basin*  
609 *Research* 8, 29-44.

610 Huisink, M., 1997. Late glacial sedimentological and morphological changes in a  
611 lowland river in response to climate change: the Maas, southern Netherlands. *Journal*  
612 *of Quaternary Science* 12, 209-223.

613 Huisink, M., 1999. Late glacial sediment budgets in the Maas Valley, The Netherlands.  
614 *Earth Surface Processes and Landforms* 24, 93-109.

615 Humphrey, N.F., Heller, P.L., 1995. Natural oscillations in coupled geomorphic  
616 systems: an alternative origin for cyclic sedimentation. *Geology* 23, 499–502.

617 Jackson, J., Haines, A.J., Holt, W.E., 1995. The accommodation of Arabia-Eurasia  
618 plate convergence in Iran. *Journal of Geophysical Research* 100, 15205-15209.

619 Jamali, F., Hessami, K., Ghorashi, M., 2011. Active tectonics and strain partitioning  
620 along dextral fault system in Central Iran: Analysis of geomorphological observations  
621 and geophysical data in the Kashan region. *Journal of Asian Earth Sciences* 40, 1015-  
622 1025.

623 Jones, S.J., 2004. Tectonic controls on drainage evolution and development of terminal  
624 alluvial fans, southern Pyrenees, Spain. *Terra Nova* 16, 121-127.

625 Jones, S.J., Frostick, L.E., Astin, T.R., 1999. Climatic and tectonic controls on fluvial  
626 incision and aggradation in the Spanish Pyrenees. *Journal of the Geological Society*  
627 156, 761-769.

628 Jones, S.J., Frostick, L.E., Astin, T.R., 2001. Braided stream and flood plain  
629 architecture: The Río Vero Formation, Spanish Pyrenees. *Sedimentary Geology* 139,  
630 229-260.

631 Kehl, M., 2009. Quaternary climate change in Iran: the state of knowledge. *Erdkunde*,  
632 63, 1-17.

633 Klinger, Y., Avouac, J.P., Bourles, D., Tisnerat, N., 2003. Alluvial deposition and lake-  
634 level fluctuations forced by Late Quaternary climate change: the Dead Sea case  
635 example. *Sedimentary Geology* 162, 119-139.

636 Kober, F., Zeilinger, G., Dolati, A., Smit, J., Ivy-Ochs, S., Kubik, P.W., 2013 Temporal  
637 calibration of fluvial sequences in the Makran Range, SE-Iran. *Global and Planetary*  
638 *Change* 111, 133-149.

639 Le Dortz, K., Meyer, B., Sebrier, M., Nazari, H., Braucher, R., Fattahi, M., Benedetti,  
640 L., Foroutan, M., Siame, L., Bourles, D., Talebian, M., Bateman, M.D., Ghoraiishi,

641 M., 2009, Holocene right-slip rate determined by cosmogenic and OSL dating on the  
642 Anar fault, central Iran. *Geophysical Journal International* 179, 700–710.

643 Le Dortz, K., Meyer, B., Sébrier, M., Braucher, R., Nazari, H., Benedetti, L., Fattahi,  
644 M., Bourles, D., Foroutan, M., Siame, L., Rashidi, A., Bateman, M.D., 2011. Dating  
645 inset terraces and offset fans along the Dehshir fault combining cosmogenic and OSL  
646 methods. *Geophysical Journal International* 185, 1147-1174.

647 Leeder, M.R., Mack, G.H., 2001. Lateral erosion ("toe-cutting") of alluvial fans by  
648 axial rivers; implications for basin analysis and architecture. *Journal of the Geological*  
649 *Society of London* 158, 885-893.

650 Leleu, S., Ghienne, J-F., Manatschal, G., 2009. Alluvial fan development and morpho-  
651 tectonic evolution in response to contractional fault reactivation (Late Cretaceous-  
652 Palaeocene), Provence, France. *Basin Research* 21, 157-187.

653 Lin, C., Eriksson, K., Sitian, L., Yongxian, W., Jianye, R., Yanmei, Z., 2001. Sequence  
654 architecture, depositional systems, and controls on development of lacustrine basin  
655 fills in part of the Erlian Basin, Northeast China. *American Association of Petroleum*  
656 *Geologists Bulletin* 85, 2017-2043.

657 Mack, G.H., Leeder, M.R., 1999. Climatic and tectonic controls on alluvial fan and  
658 axial-fluvial sedimentation in the Plio-Pleistocene Palomas half graben, southern Rio  
659 Grande Rift. *Journal of Sedimentary Research* 69, 635-652.

660 Magee, J.W., Miller, G.H., Spooner, N.A., Questiaux, D., 2004. Continuous 150 k.y.  
661 monsoon record from Lake Eyre, Australia: insolation-forcing implications and  
662 unexpected Holocene failure. *Geology* 32, 885-888.

663 Maggi, A., Priestley, K., 2005. Surface waveform tomography of the Turkish-Iranian  
664 plateau. *Geophysical Journal International* 160, 1068-1080.

665 Meyer, B., Mouthereau, F., Lacombe, O., Agard, P., 2006. Evidence of Quaternary  
666 activity along the Deshir fault: implication for the Tertiary tectonics of central Iran.  
667 *Geophysical Journal International* 164, 192-201.

668 Morley, C.K., Kongwung, B., Julapour, A.A., Abdolghafourian, M., Hajian, M.,  
669 Waples, D., Warren, J., Otterdoom, H., Srisuriyon, K., Kazemi, H., 2009. Structural  
670 development of a major late Cenozoic basin and transpressional belt in central Iran:  
671 The Central Basin in the Qom-Saveh area. *Geosphere* 5, 325–362.

672 Motamed, A., 1997. Quaternary. University of Tehran, Publication, 328p.

673 Nadimi, A., Konon, A., 2012. Gaw-Khuni Basin: An active stepover structure in the  
674 Sanandaj-Sirjan zone, Iran. *Geological Society of America Bulletin* 124, 484-498.

675 Nazari, H., Fattahi, M., Meyer, B., Sébrier, M., Talebian, M., Foroutan, M., Le Dortz,  
676 K., Bateman, M.D., Ghorashi, M., 2009. First evidence for large earthquakes on the  
677 Deshir Fault, Central Iran Plateau. *Terra Nova* 21, 417-426.

678 Nissen, E., Tatar, M., Jackson, J.A., Allen, M.B., 2011. New views on earthquake  
679 faulting in the Zagros fold-and-thrust belt of Iran. *Geophysical Journal International*  
680 186, 928-944.

681 Owen, R.B., Renault, R.W., 1986. Sedimentology, stratigraphy and palaeoenvironments  
682 of the Holocene Galana Boi Formation, NE Lake Turkana, Kenya. In: Frostick, L.E.,  
683 Renault, R.W., Reid, I., Tiercelin, J.J. (Eds), *Sedimentation in the African rifts*,  
684 Geological Society of London Special Publication 25, pp 311-322.



685 Parsons, B., Wright, T., Rowe, P., Andrews, J., Jackson, J., Walker, R., Khatib, M.,  
686 Talebian, M., Bergman, E., Engdahl, E.R., 2006. The 1994 Sefidabeh (eastern Iran)  
687 earthquakes revisited: new evidence from satellite radar interferometry and carbonate  
688 dating about the growth of an active fold above a blind thrust fault. *Geophysical*  
689 *Journal International* 164, 202-217.

690 Paul, A., Hatzfeld, D., Kaviani, A., Tatar, M., Péquegnat, C., 2010. Seismic imaging of  
691 the lithospheric structure of the Zagros mountain belt (Iran). In: Leturmy, P., Robin,  
692 C. (Eds), *Tectonic and Stratigraphic Evolution of Zagros and Makran during the*  
693 *Mesozoic–Cenozoic*. Geological Society of London Special Publication 330, pp 5-18.

694 Pope, R.J.J., Wilkinson, K.N., 2005. Reconciling the roles of climate and tectonics in  
695 Late Quaternary fan development on the Spartan piedmont, Greece. In: Harvey, A.M.,  
696 Mather, A.E., Stokes, M. (Eds), *Alluvial Fans: Geomorphology, Sedimentology,*  
697 *Dynamics*, Geological Society, Special Publications 251, pp 133–152.

698 Preusser, F., 2009. Chronology of the impact of Quaternary climate change on  
699 continental environments in the Arabian Peninsula. *Comptes Rendus Geoscience* 341,  
700 621–632.

701 Quigley, M.C., Sandiford, M., Cupper, M.L., 2007. Distinguishing tectonic from  
702 climatic controls on range-front sedimentation. *Basin Research*, 19, 491-505.

703 Regard, V., Bellier, O., Braucher, R., Gasse, F., Bourles, D., Mercier, J., Thomas, J.-C.,  
704 Abbassi, M.R., Shabanian, E., Soleymani, Sh., 2006.  $^{10}\text{Be}$  dating of alluvial deposits  
705 from southeastern Iran (the Hormoz Strait area). *Palaeogeography, Palaeoclimatology,*  
706 *Palaeoecology* 242, 36-53.

707 Schick, A.P., Lekach, J., 1987. A high magnitude flood in the Sinai desert. In: Mayer,  
708 L., Nash, D. (Eds), Catastrophic flooding, Allen and Unwin, Boston, pp. 381-410.

709 Schmidt, A., Quigley, M., Fattahi, M., Azizi, G., Maghsoudi, M., Fazeli, H., 2011.  
710 Holocene settlement shifts and palaeoenvironments on the Central Iranian Plateau:  
711 investigating linked systems. *The Holocene* 21, 583-595.

712 Scotese, C.F., McKerrow, W.S., 1990. Revised world maps and introduction. In:  
713 McKerrow, W.S., Scotese C.F. (Eds), *Palaeozoic Palaeogeography and*  
714 *Biogeography*. Geological Society, London, Memoir 12, pp 1-21.

715 Sözbilir, H., Sari, B., Uzel, B., Sümer, Ö., Akkiraz, S., 2011. Tectonic implications of  
716 transtensional supradetachment basin development in an extension parallel transfer  
717 zone: The Kocayağ Basin, western Anatolia, Turkey. *Basin Research* 23, 423-448.

718 Stainstreet, I.G., McCarthy, T.S., 1993. The Okavango Fan and the classification of  
719 subaerial fan systems. *Sedimentary Geology* 8, 115-133.

720 Stampfli, G.M., Marcoux, J., Baud, A., 1991. Tethyan margins in space and time. In:  
721 Channell, J.E.T., Winterer, E.L., Jansa, L.F. (Eds), *Paleogeography and*  
722 *Paleoceanography of the Tethys*. *Palaeogeography, Palaeoclimatology, Palaeoecology*  
723 87, 373–410.

724 Stevens, L.R., Ito, E., Schwab, A., Wright, H.E., 2006. Timing of atmospheric  
725 precipitation in the Zagros Mountains inferred from a multi-proxy record from Lake  
726 Mirabad, Iran. *Quaternary Research* 66, 494-500.

727 Talebian, M., Tabatabaei, S.H., Fattahi, M., Ghorashi, M., Beitollahi, A.,  
728 Ghalandarzadeh, A., Riahi, M.A., 2010. Estimating slip rates of faults around Bam

729 and their application in Evaluation of earthquake hazard. *Geosciences* 19, 149-156 (in  
730 Farsi, with English abstract).

731 Vázquez-Urbez, M., Arenas, C., Pardo, G., Pérez-Rivarés, J., 2013. The Effect of  
732 Drainage Reorganization and Climate On the Sedimentologic Evolution of  
733 Intermontane Lake Systems: The Final Fill Stage of the Tertiary Ebro Basin (Spain).  
734 *Journal of Sedimentary Research* 83, 562-590.

735 Vermoere, M., Degryse, P., Vanhecke, L., Muchez, P.H., Paulissen, E., Smets, E.,  
736 Waelkens, M., 1999. Pollen analysis of two travertine sectors in Basköy  
737 (southwestern Turkey): implications for environmental conditions during the Early  
738 Holocene. *Review of Palaeobotany and Palynology* 105, 93-110.

739 Vernant, P., Nilforoushan, F., Hatzfeld, D., Abbassi, M., Vigny, C., Masson, F.,  
740 Nankali, H., Martinod, J., Ashtiani, A., Bayer, R., Tavakoli, F., Chery, J., 2004.  
741 Contemporary crustal deformation and plate kinematics in Middle East constrained  
742 by GPS measurements in Iran and northern Iran. *Geophysical Journal International*  
743 157, 381-398.

744 Viseras, C., Calvache, M.L. Soria, J.M., Fernandez, C.J., 2003. Differential features of  
745 alluvial fans controlled by tectonic or eustatic accommodation space. Examples from  
746 the Betic Cordillera, Spain. *Geomorphology* 50, 181-202.

747 Walker, R.T., Talebian, M., Sloan, R.A., Rasheedi, A., Fattahi, M., Bryant, C., 2010.  
748 Holocene slip-rate on the Gowk strike-slip fault and implications for the distribution  
749 of tectonic strain in eastern Iran. *Geophysical Journal International* 181, 221-228.

750 Walker, R.T., Fattahi, M., 2011. A framework of Holocene and Late Pleistocene  
751 environmental change in eastern Iran inferred from the dating of periods of alluvial  
752 fan abandonment, river terracing, and lake deposition. *Quaternary Science Reviews*  
753 30, 1256-1271.

754 Wasylikowa, K., Witkowski, A., Walanus, A., Hutorowicz, A., Alexandrowicz, S.W.,  
755 Langer, J.J., 2006. Palaeolimnology of Lake Zeribar, Iran, and its climatic  
756 implications. *Quaternary Research* 66, 477-493.

757 Waters, J.V., Jones, S.J., Armstrong, H.A., 2010. Climatic controls on late Pleistocene  
758 alluvial fans, Cyprus. *Geomorphology* 115, 228-251.

759

760

761 **Table and Figure Captions**

762 Table 1

763 Summary morphometric characteristics of the studied fluvial fans along the Kohrud  
764 mountain belt, central Iran.

765

766 Table 2

767 Available age constraints from alluvial fan abandonment and playa lake sediments  
768 across the central Iranian plateau. Details of the age dating methods used can be found  
769 within the papers referenced.

770

771 Fig. 1. (a) Neotectonic map of Iran, after Allen et al. (2011). Q-Z = Qom-Zefreh Fault.  
772 (b) Location map for (a). Thick white line is the approximate boundary of the Turkish-  
773 Iranian plateau. Dashed lines mark basement block boundaries within Iran. CIM -  
774 Central Iranian Microcontinent; DSFS – Dead Sea Fault System; EAF – East Anatolian  
775 Fault; NAF – North Anatolian Fault. (c) Cenozoic tectonic units of Iran. The extent of  
776 Central Iran is shown by hatching between the Zagros suture and the southern side of  
777 the Alborz (solid lines).

778 Fig. 2. Geological map of the central part of the Kohrud mountain belt and the  
779 Meymeh-Esfahan basin. The active Qom-Zefreh and Deshir right lateral faults cut  
780 across the Kohrud mountain belt, juxtaposing Palaeozoic-Mesozoic sediments against  
781 Eocene volcanic rocks. Alluvial fans drain the Kohrud mountain belt into both the  
782 Zavareh and Gavkhoni playa lakes. The boxes outline the areas enlarged of Landsat

783 mosaics in figures 5 and 6. Alluvial fans identified with cross-hatching are those  
784 specifically included in this study and from the NW to SE they are the Soh, Zefreh and  
785 Feshark fans respectively.

786 Fig. 3. View north towards the apex of the Feshark fan showing the typical gradient of  
787 the fans draining the Kohrud mountain belt (see Table 1) and the margin of the  
788 Meymeh-Easfahan basin delimited by the Qom-Zefreh fault. Distance between pylons  
789 is 100 m.

790 Fig. 4. Catchment area versus fan area for 35 fans along the northern faulted margin of  
791 Meymeh-Esfahan basin.

792 Fig. 5. Landsat Mosaic of the Soh fluvial fan and smaller adjoining fans along the  
793 margin of the Meymeh-Esfahan basin. Dashed line refers to long profile as in Figure 7.  
794 Note the first fan phase, which is now characteristically deeply incised. The fan  
795 sediments are cemented with hot-spring travertines and incorporate large travertine  
796 clasts, that are considered to be late Pleistocene in age (Arzani, 2012).

797 Fig. 6. Landsat Mosaic of the Zefreh and Feshark fluvial fans. Dashed lines refer to  
798 long profiles as in Figure 7. Black arrows identify the former Govkhoni playa lake high  
799 stand. The catchment for both fans is within Eocene basic volcanics. Note the sharp  
800 contact between the fans and Eocene volcanics of the catchment area. This is delimited  
801 by the Qom-Zefreh fault.

802 Fig. 7. Long profiles of the Soh, Zefreh and Feshark fans draining the Kohrud mountain  
803 belt showing the position of the mountain front, marking the faulted boundary with the  
804 northern margin of the Meymeh-Esfahan basin (see Figs. 5, 6 for location of profiles).

805 In the case of the Zefreh and Feshark fans the mountain front is delimited by the Qom-  
806 Zefreh fault.

807 Fig. 8. Detailed sedimentary logs for the Soh fan. The position of the sedimentary logs  
808 is located on the inset map. Sedimentary logs 2 and 3 contain intercalated travertine  
809 deposits, recording episodes of fault activity that controlled deposition through CO<sub>2</sub>-  
810 rich thermal mineral waters as the fan crosses a fault. Sedimentary logs 4, 5 and 6  
811 record abrupt alternation of coarse fan and playa lake margin sediments in the distal  
812 reaches of the alluvial fan. This is also common to the Zefreh and Feshark fans.

813 Fig. 9. Field photographs of alluvial fan sediments. (A) View eastwards across the  
814 surface of the Zefreh fan. Bimodal distribution of cobble and pebble size clasts in the  
815 proximal portions. (B) Zefreh and Feshark fans dominated by Eocene alkali volcanic  
816 clasts, with minor Mesozoic limestone and sandstone clasts. Scale shown on ruler in  
817 centimetres. (C) Pebble to small cobble size clast supported gravels that fine upwards  
818 into coarse-grained sands. The fining upwards gravel occur as ~30cm repeating  
819 packages through a 2 m trench cut perpendicular to flow across the Feshark fan.

820 Fig. 10. Graph illustrating the relationship between the proportion of fan or playa lake  
821 sediments and the distance from the apex for the Soh, Zefreh and Feshark fans.

822 Fig. 11. Field photographs of hot-spring travertines. (A) Example of layered mat facies  
823 with some banded white veins, proximal portion of the Soh fan. Dense aragonite veins  
824 that are composed of bands of white crystals cut through the layered mats. These white  
825 banded veins mainly range in thickness from 5 cm to 50 cm and would have been  
826 precipitated from rapid degassing of CO<sub>2</sub> from highly agitated subsurface waters while

827 the travertines were still an *in-situ* mound. (B) Layered mat facies intercalated with  
828 conglomerates, proximal Zefreh fan. Well preserved pool and rim geometries of  
829 microterraces that once formed on the margin of an active travertine mound.

830 Fig. 12. Intercalated playa lake (P) and fan (F) sediments. Fine-grained lake sediments  
831 are often superimposed onto the coarser sands and gravels frequently with gypsum  
832 crusts. The lake sediments are often rippled with minor convoluted bedding. The  
833 coarser fan sediments exhibit horizontal stratification, with some low angle planar  
834 cross-bedding, pebble imbrication and erosional bases. The intercalation of sediments  
835 are found throughout the distal portion of the Zefreh and Feshark fans and can be  
836 identified along the Gavkhouni high stand strand line (See Fig. 6).

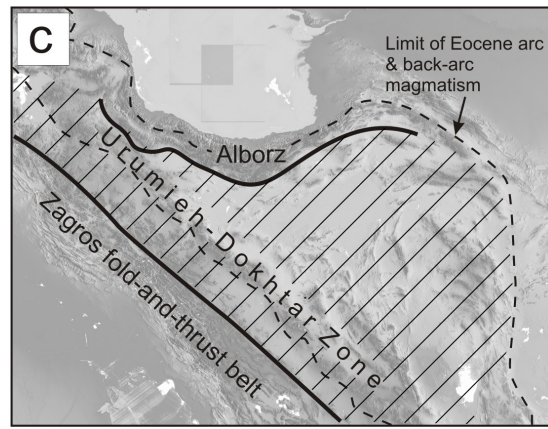
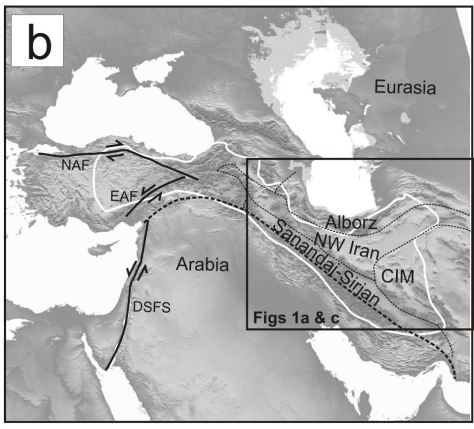
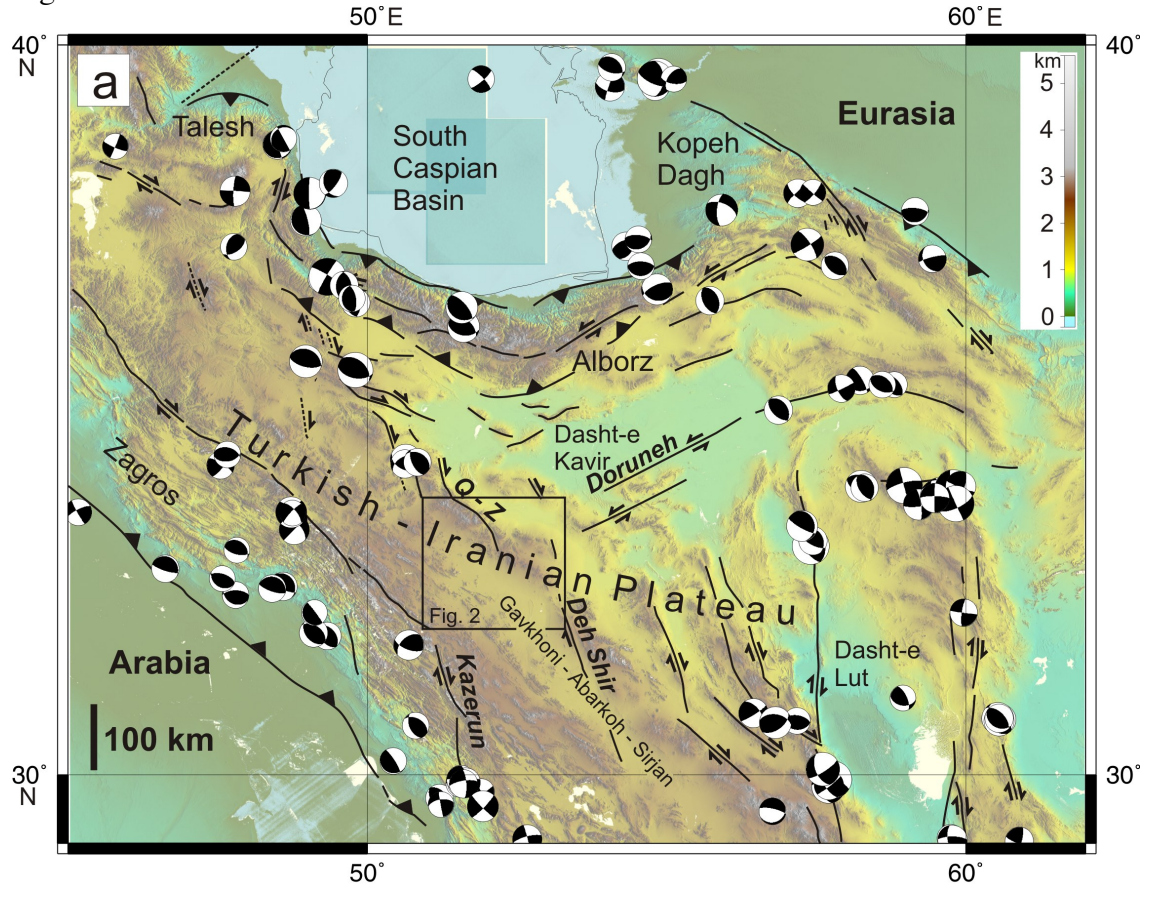
837 Fig. 13. Detailed sedimentary log of the distal portion of the Zefreh fan. See figures 2  
838 and 6 for location.  $D_{90}$  records the 90<sup>th</sup> percentile of the coarsest grain size fraction.

839 Fig. 14. Field photograph of view southwards across the Gavkhoni playa. In the  
840 foreground, is a discrete patch of white anhydrite-glauberite surrounded by brown clay.  
841 This is a common occurrence across the modern Gavkhoni playa.

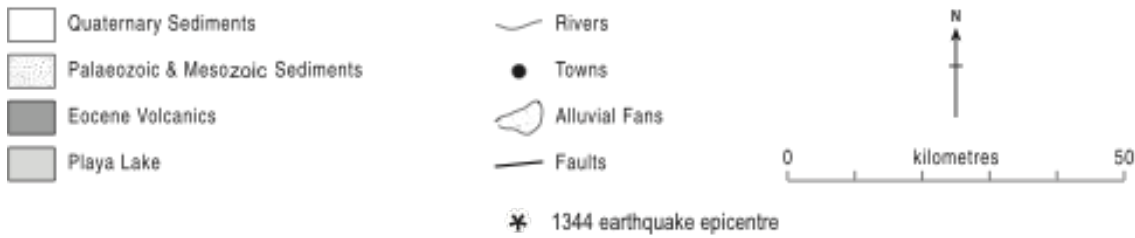
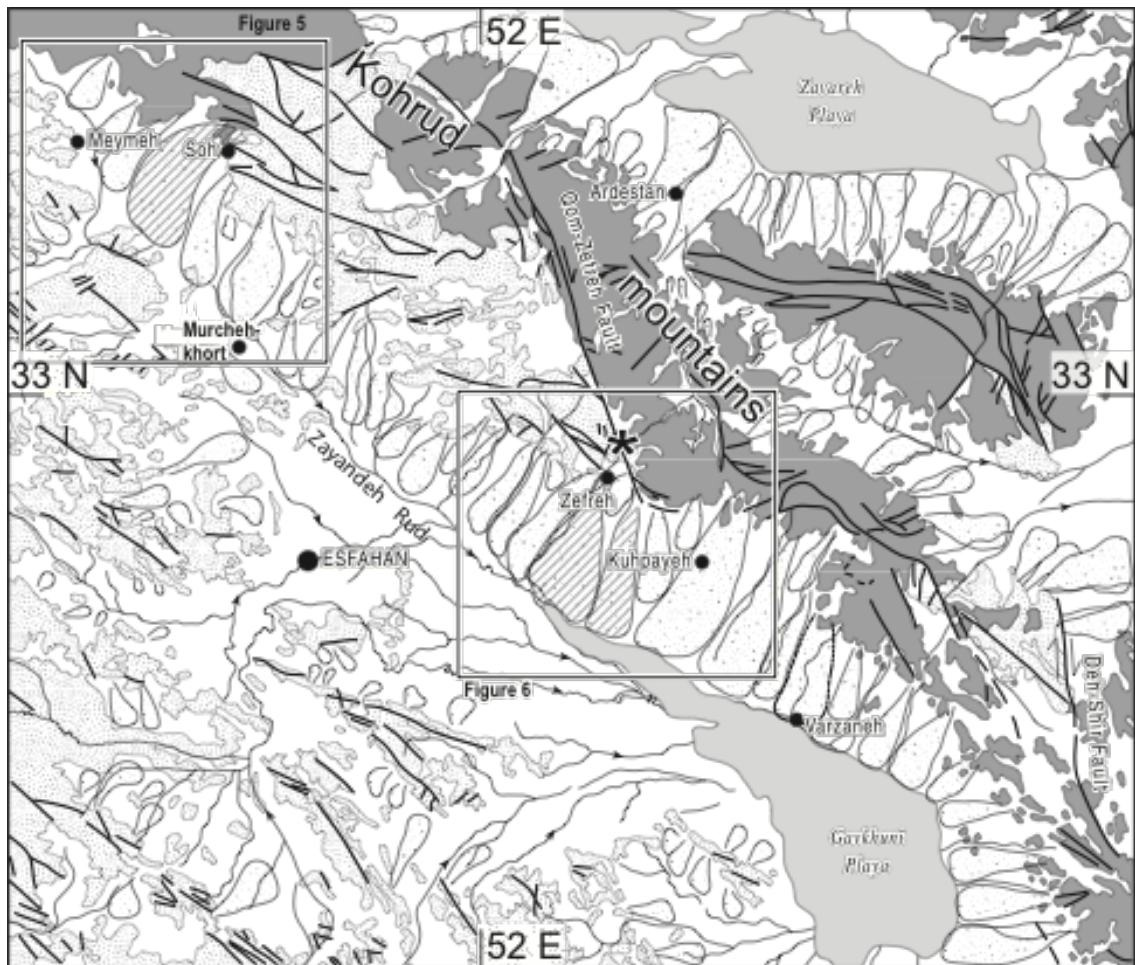
842  
843  
844  
845  
846  
847  
848  
849  
850  
851  
852  
853  
854  
855  
856  
857



858 Figure 1



859



860

861 Figure 2

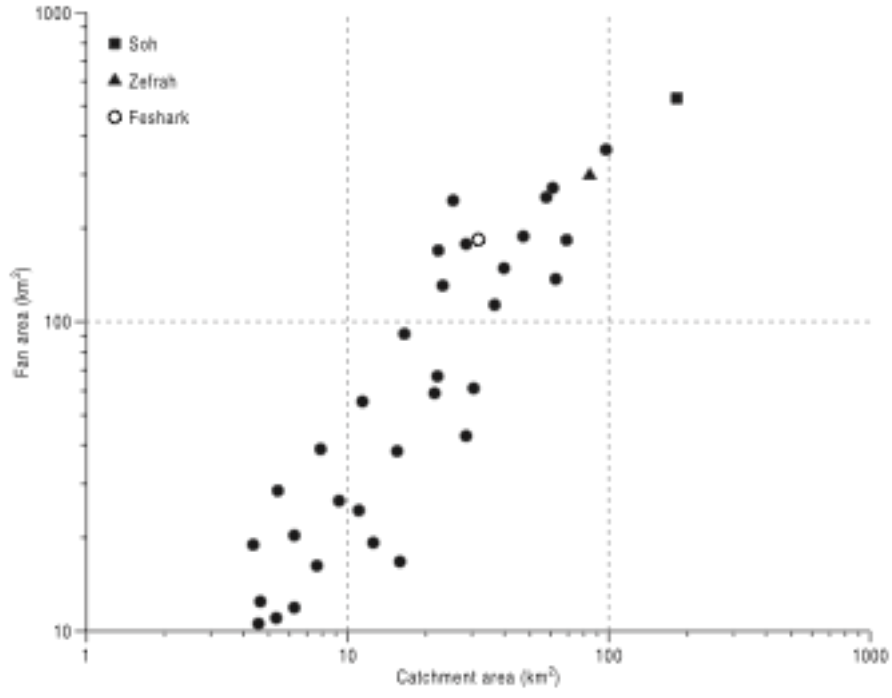




862

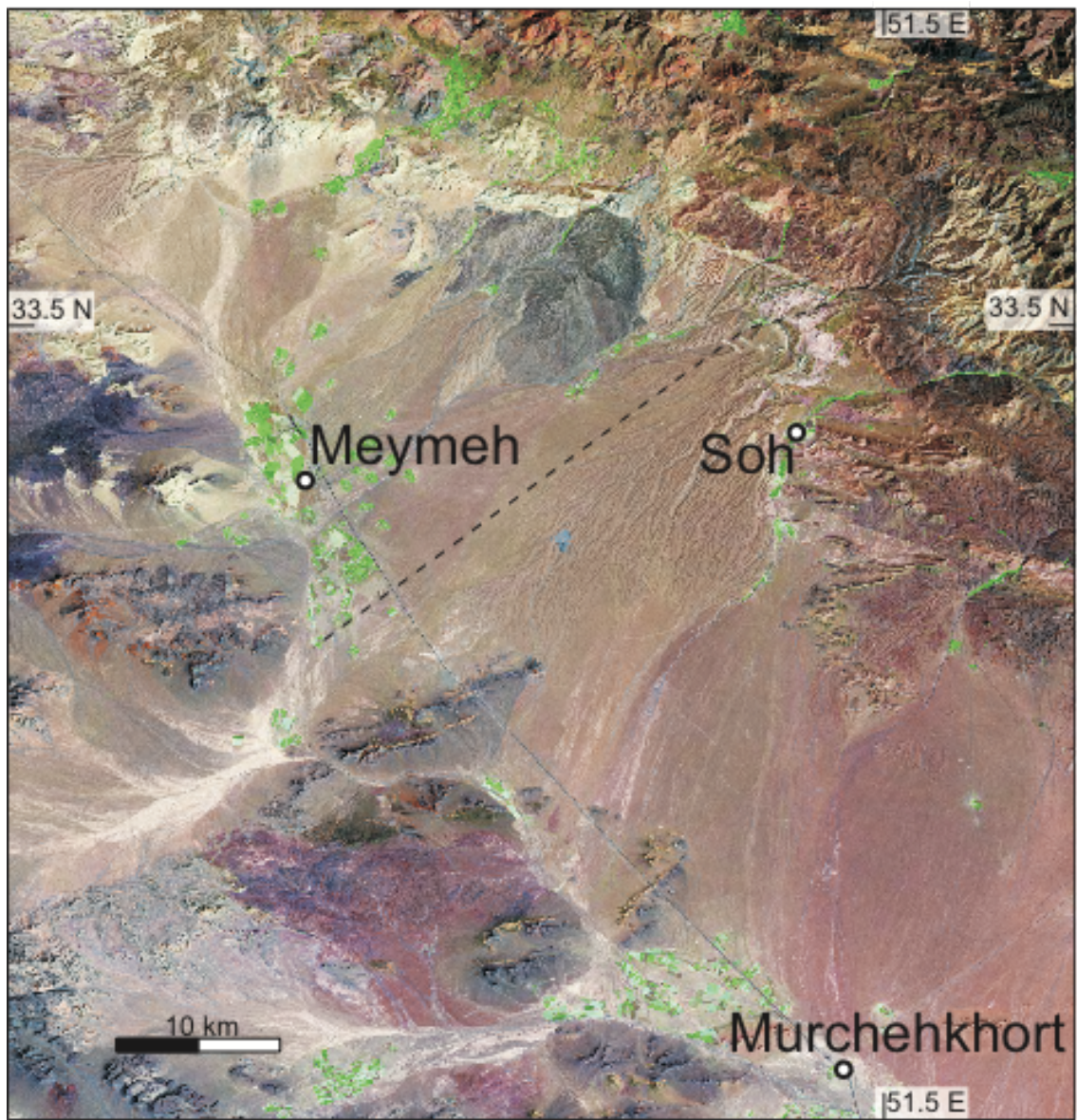
863

864 Figure 3



865

866 Figure 4

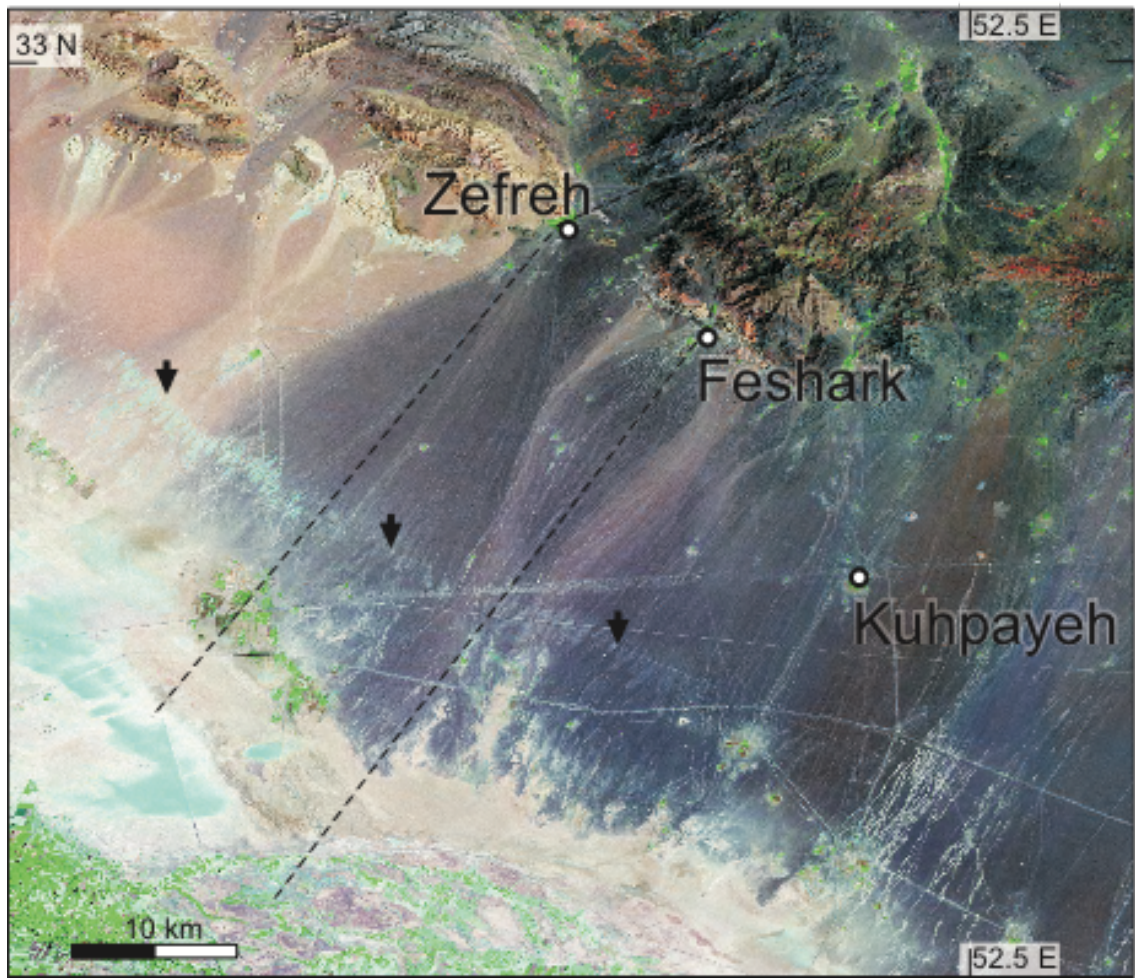


867

868

869 Figure 5

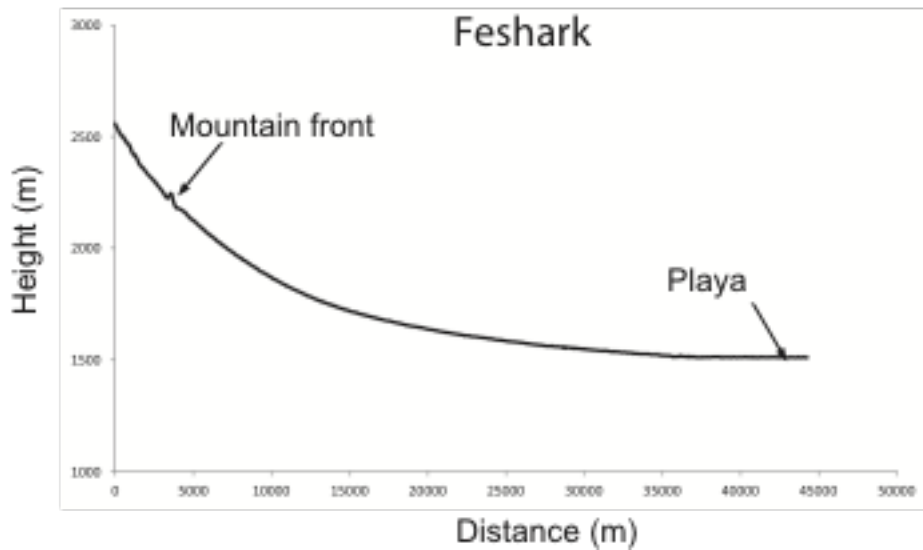
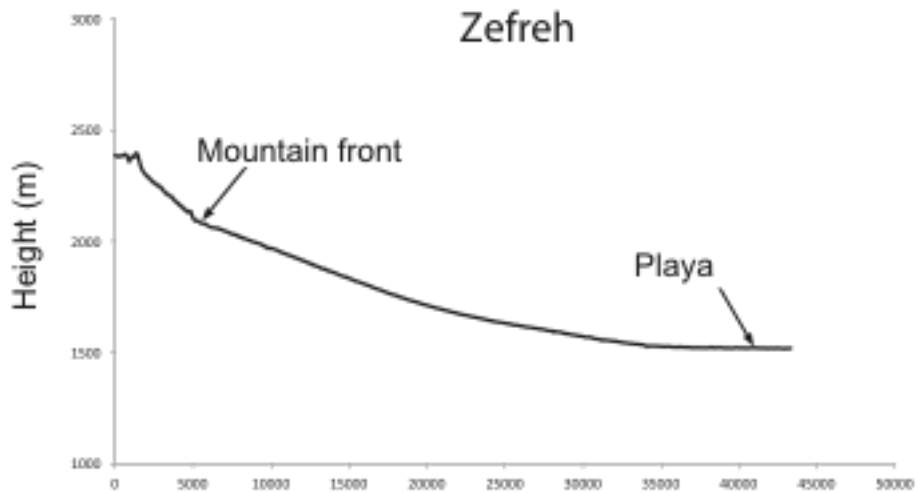
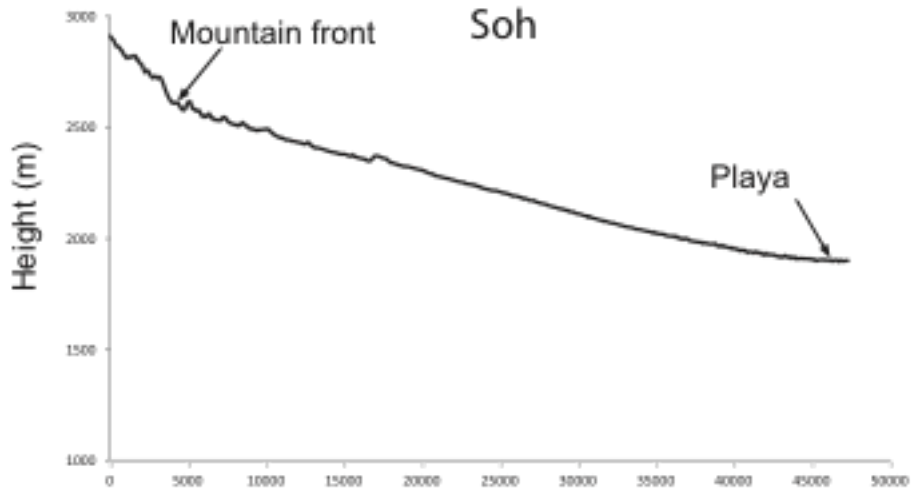


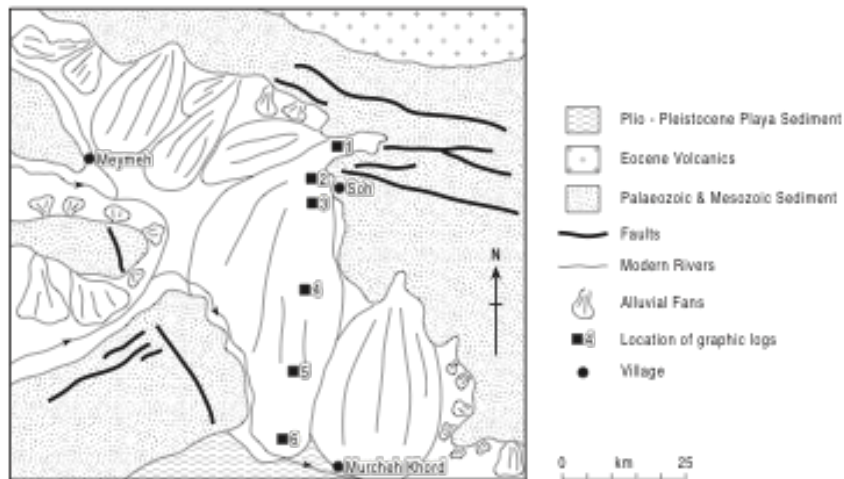
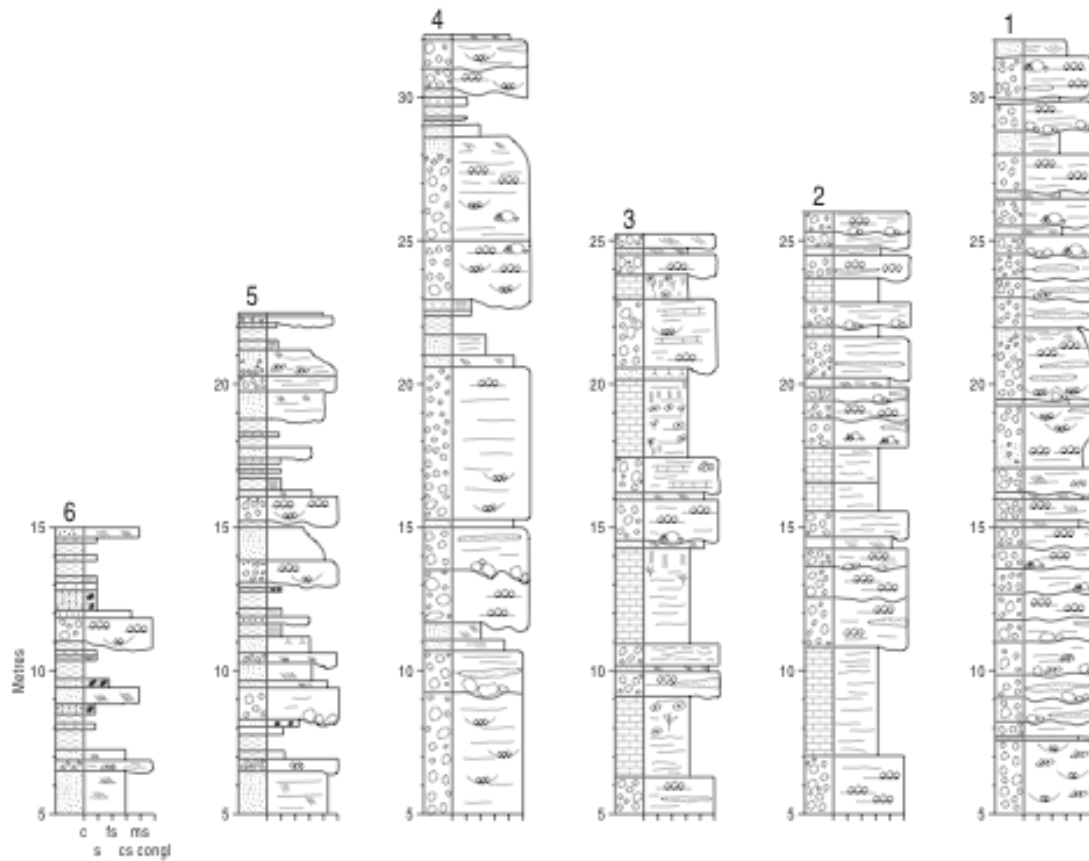


870

871

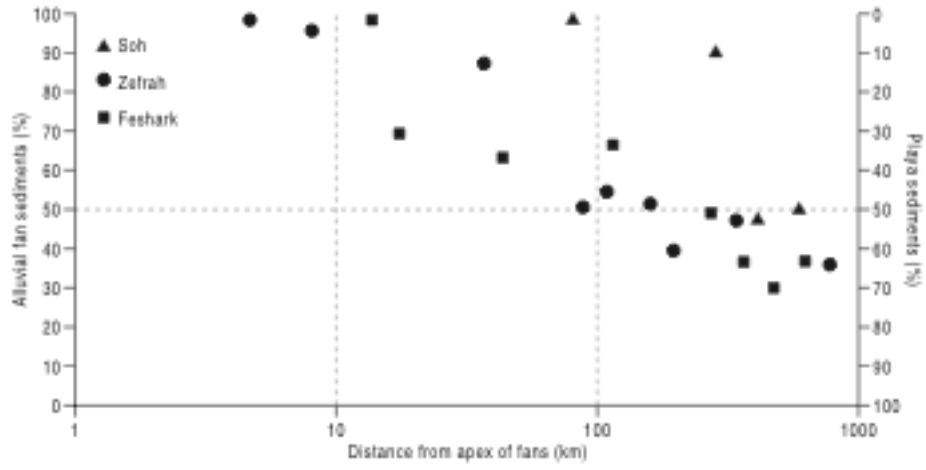
872 Figure 6









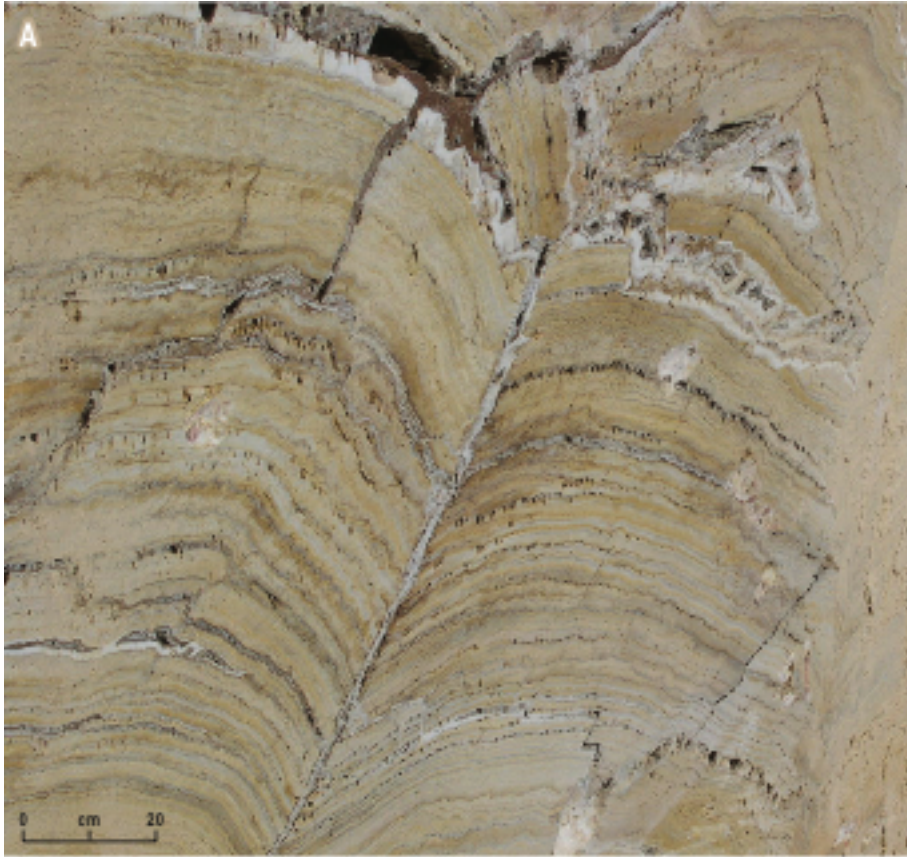


876

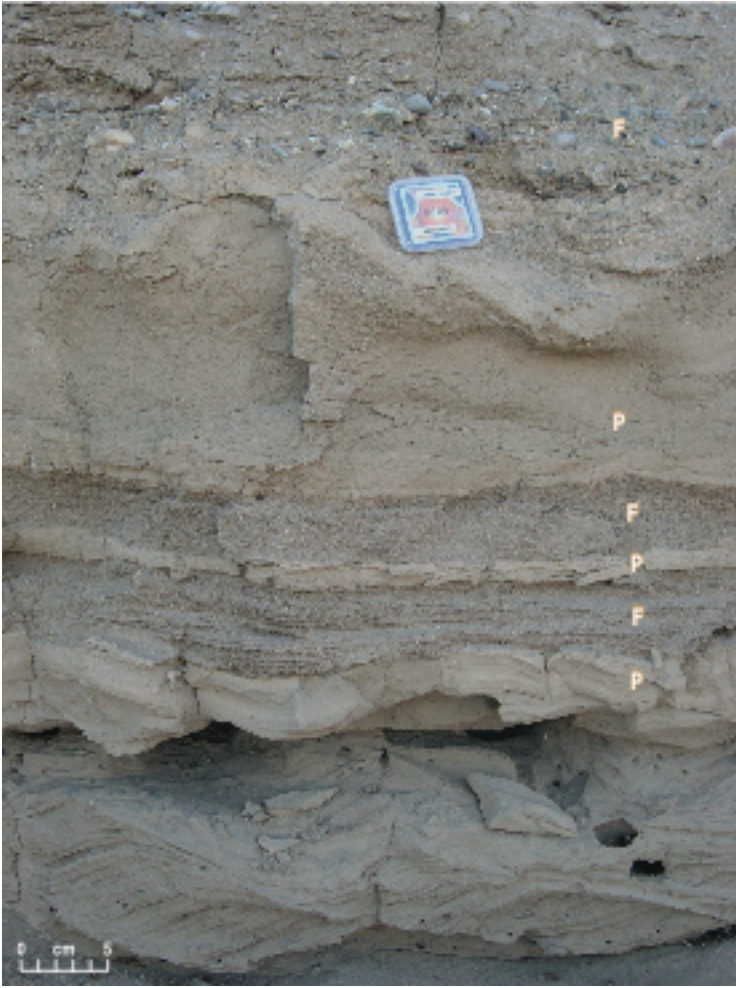
877

878 Figure 10



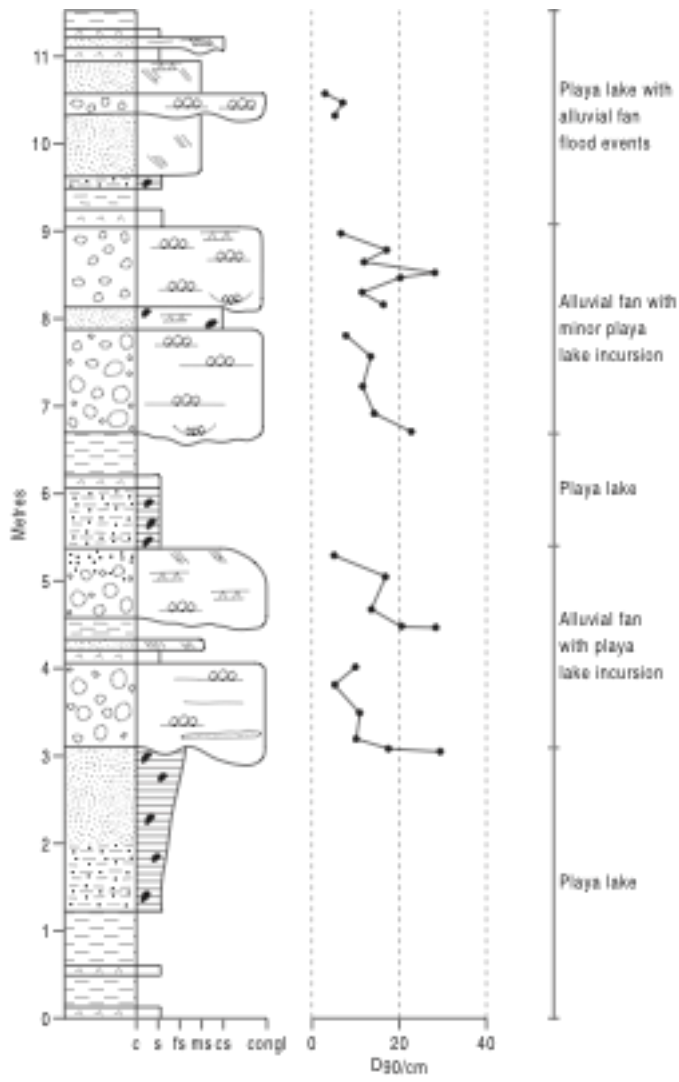


879



880

881 Figure 12



882

883 Figure 13





884

885

886 Figure 14

| Parameters                          | Soh  | Zefreh   | Feshark  |
|-------------------------------------|--|--|--|
| Fan area (km <sup>2</sup> )         | 537  | 309  | 179  |
| Average fan slope (degrees)         | 0.01-0.15  | 0.04-0.2   | 0.06-0.23  |
| Average catchment slope (degrees)   | 0.48   | 0.39   | 0.39   |
| Fan progradation distance (km)      | 32.4   | 35.6   | 28.3   |
| Fan radius (km)                     | 8.1  | 6.3  | 3.7  |
| Catchment area (km <sup>2</sup> )   | 178  | 84.5   | 23.5   |
| Catchment length (km)               | 23.6   | 15.7   | 8.7  |
| Catchment maximum elevation (m asl) | 3200   | 3250   | 3200   |
| Catchment basin relief (m)          | 900  | 1250   | 1270   |
| Catchment lithology types           | Devonian to Cretaceous sandstones, siltstones and carbonates. Hot spring Travertines   | Predominantly Eocene andesitic volcanics. Some Hot spring travertines  | Predominantly Eocene andesitic volcanics   |
| Fan lithology types                 | Carbonate clasts (75%) sandstone and siltstone clasts (25%). Where fan intercalated with travertines, carbonates (30%), sandstones (15-20%), travertine clasts up to (50%) in proximal fan | Volcaniclastic clasts (75%) basaltic and andesitic clasts (~15%) dolomite clasts (~5%), travertine clasts only proximal fan (5%) | Volcaniclastic clasts (75%) basaltic and andesitic clasts (~15%) dolomite clasts (~5%), travertine clasts only proximal fan (5%) |

887  
888 Table 1.  
889

| Site name                               | Method used                                | Sediment type                                  | Age (ka)  | Reference             |
|---|--|--|---|-----------------------|
| South Golbah, Dasht-e-Lut, SE Iran      | $^{14}\text{C}$                            | Terrestrial wood in lake carbonates            | 7.9 +/- 0.1   | Walker et al., 2010   |
| Anar, Central Iran                      | OSL/ $^{10}\text{Be}$                      | Alluvial fan sediments                         | 11.8 +/- 6.5  | Le Dortz et al., 2009 |
| Dehshir and Marvast River, Central Iran | OSL/ $^{10}\text{Be}$ and $^{26}\text{Cl}$ | Alluvial fan sediments and river terraces      | 412 (oldest terrace);<br>26.9+/-1.3;<br>21.9+/-1.5;<br>10.0+/-0.6 | Le Dortz et al., 2011 |
| Gavkhouni, Central Iran                 | OSL  | Paleosols and playa sediments                  | 9.6 +/- 2.4   | Ayoubi, 2002          |
| Dehshir, Central Iran                   | OSL  | Alluvial fan and fluvial                       | 2.8+/-1.4;<br>older terraces<br>10-30                             | Nazari et al., 2009   |
| Bam, Dasht-e-Lut, SE Iran               | IRSL                                       | Sands and silts of alluvial fan                | 9.2 +/- 1.5   | Talebian et al., 2010 |
| Hajiarb Fan, NW Iran                    | OSL  | Alluvial fan sediments                         | 8.83 +/- 2.84   | Schmidt et al., 2011  |
| Sefidabeh, Eastern Iran                 | U-series                                   | Calcite cemented sandstones from fan sediments | 99 +30/-24  | Parsons et al., 2006  |